Successful treatment of JAK1 associated inflammatory disease

Antoine Fayand, Véronique Hentgen, Céline Posseme, Carole Lacout, Capucine Picard, Philippe Moguelet, Margaux Cescato, Nabiha Sbeih, Thomas R.J. Moreau, Yixiang Yj. Zhu, et al.

Successful treatment of *JAK1* associated inflammatory disease

Antoine Fayand [1,21] MD, Véronique Hentgen [2*] MD, Céline Posseme Ph.D [3*] ,Carole Lacout[4,21*] MD, Capucine Picard[5] MD, Ph.D, Philippe Moguelet[6] MD, Margaux Cescato[1] M.Sc, Nabiha Sbeih[7] MD, Thomas R.J. Moreau[1] M.Sc, Yixiang YJ Zhu[1] M.Sc, Jean-Luc Charuel[8] MD, Aurélien Corneau[9] Ph.D, Joelle Deibener-Kaminsky[10] MD, Stéphanie Dupuy[11] Ph.D, Mathieu Fusaro[5] MD, Benedicte Hoareau[9] M.Sc, Alain Hovnanian[12,13] MD, Ph.D, Vincent Langlois[14], Laurent Le Corre[15], Thiago T Maciel[7] Ph.D, Snaigune Miskinyte[12] M.Sc, Makoto Miyara[8,16] MD, Ph.D, Thomas Moulinet[10] MD, Magali Perret[17] MD, Marie Hélène Schuhmacher[18] MD, Rachel Rignault-Bricard[7] , Ph.D, Sébastien Viel[13] MD, Ph.D, Angélique Vinit [9] M.Sc , Angèle Soria[19] MD, Ph.D, Darragh Duffy[3] Ph.D, Jean-Marie Launay[20] MD, Ph.D, Jacques Callebert[20] MD, Ph.D, Jean Philippe Herbeuval[1] Ph.D, Mathieu P Rodero[1§] Ph.D, Sophie Georgin-Lavialle[21§†] MD, Ph.D.

[1] Université Paris Cité, CNRS, Laboratoire de Chimie et de Biochimie Pharmacologiques et Toxicologiques, F-75006 Paris, France
[2] Pediatric Infectious Disease Group (GPIP), Créteil, France;
Department General Pediatrics, Centre Hospitalier de Versailles, Le Chesnay, France.
[3] Translational Immunology Unit, Institut Pasteur, Université de Paris Cité, Paris, France
[4] Sorbonne University, Genetic Laboratory, Assistance Publique - Hôpitaux de Paris (APHP), Trousseau Hospital, Paris, France.
[5] Study Center for Primary Immunodeficiencies, APHP, Necker Hospital for Sick Children, Université de Paris Cité, Paris, France.
[6] Department of Pathology, Sorbonne University, Tenon Hospital, APHP, Paris, France.
[7] Laboratory of Cellular and Molecular Mechanisms of Hematological Disorders and Therapeutical Implications, Université Paris Cité, Imagine Institute, Inserm U1163, Paris, France
[8] Groupement Hospitalier Pitié-Salpêtrière APHP, Département of immunology, Paris, France.
[9] Sorbonne Université, UMS037, PASS, Plateforme de Cytométrie de la Pitié-Salpêtrière CyPS, Paris, France.
[10] Department of Internal Medicine and Clinical Immunology, Nancy University Hospital, 5 Rue du Morvan, Vandoeuvre-lès-Nancy 54500, France; UMR 7365, IMoPA, University of Lorraine, CNRS, Nancy, France.
[11] BioMedTech Facilities INSERM US36 - CNRS UAR2009 - Université Paris Cité, France.
[12] INSERM UMR1163, Laboratory of genetic skin diseases, Imagine Institute, University Paris Cité, Paris, France.
[13]Department of Genomics Medicine of Rare Diseases, Hôpital Necker Enfants Malades, AP-HP, Paris, France.
[14] Department of Internal Medicine, Jacques Monod Hospital, Le Havre, France.
[15] Université de Paris Cité, CNRS, UMR8601, LCBPT, Macromolecular Modeling Platform, Paris, France.
[16] Inserm U1135, Centre d'Immunologie et des Maladies Infectieuses (CIMI-Paris), Hôpital Pitié-Salpêtrière, AP-HP, Sorbonne Université, Paris, France
[17] Immunology Laboratory, Lyon Sud Hospital, Hospices Civils de Lyon, University of Claude Bernard-Lyon 1, Lyon, France.
[18] Department of Internal Medicine, Emile Durkheim Hospital, Épinal, France.
[19] Tenon Hospital, Dermatology-Allergology Department, Sorbonne University, Paris, France.
[20] Service of Biochemistry and Molecular Biology, INSERM U942, Hospital Lariboisière, APHP, Paris, France.

[21] Sorbonne Université, APHP, Tenon Hospital, department of internal medicine, Paris, France.

***** Contributed equally
§ Codirected the study

[†] Corresponding author: Sophie Georgin-Lavialle: Sorbonne Université, APHP, Tenon hospital, Department of Internal Medicine, National reference center for autoinflammatory diseases and inflammatory amyloidosis (CEREMAIA), Paris, France.
sophie.georgin-lavialle@aphp.fr

Dr Hentgen and Dr Georgin-Lavialle declare no conflict of interest in relation to this manuscript. They have consultancy or speaking activities for SOBI and Novartis not related to this work. The rest of the authors declare that they have no relevant conflicts of interest.

Background: Gain of function (GOF) variants of JAK1 drive a rare immune dysregulation syndrome associated with atopic dermatitis, allergy and eosinophilia.

Objectives: To describe the clinical and immunological characteristics associated with a new GOF variant of *JAK1* and report the therapeutic efficacy of JAK inhibition.

Methods: We identified a family affected by *JAK1* associated autoinflammatory disease and performed clinical assessment and immunological monitoring on 9 patients. JAK1 signalling was studied by flow and mass cytometry in patients' cells at basal state, or after immune stimulation. A molecular disease signature in the blood was studied at the transcriptomic level. Patients were treated with one of two JAK inhibitors; either baricitinib or upadacitinib. Clinical, cellular, and molecular response were evaluated over a 2-year period.

Results: Affected individuals displayed a syndromic disease with prominent allergy including atopic dermatitis, ichthyosis, arthralgia, chronic diarrhoea, disseminated calcifying fibrous tumours and elevated whole blood histamine levels. A variant of *JAK1* localized in the pseudokinase domain was identified in all 9 affected tested patients. Hyper-phosphorylation of STAT3 was found in 5 out of 6 patients tested. Treatment of patients' cells with baricitinib controlled most of the atypical hyper-phosphorylation of STAT3. Administration of baricitinib to patients led to rapid improvement of the disease in all adults and was associated with reduction of systemic inflammation.

Conclusions: Patients with this new *JAK1* GOF pathogenic variant displayed very high levels of blood histamine and showed a variable combination of atopy with articular and gastrointestinal manifestations as well as calcifying fibrous tumours. The disease, that appears to be linked to STAT3 hyper-activation, was well controlled under treatment by JAK inhibitors in adult patients.

Clinical implication – This study significantly expands the clinical spectrum of *JAK1* associated autoinflammatory disease and report the clinical benefit of two distinct JAK inhibitors over a 2-year period in a large family.

Capsule summary– This study opens new avenues in the diagnosis and treatment of JAK1 associated autoinflammatory disease. It should help to reduce diagnostic delay of *JAK1* mutated patients.

Keywords: JAK 1, atopic dermatitis, JAK inhibitors, inborn errors of immunity, allergy

Abbreviations

CyTOF: cytometry by time of flight = mass cytometry
CT-scan: computer tomography scan
ENT: ear-nose-throat
FACS: fluorescence activated cell sorting
GOF: gain of function
IBD: inflammatory bowel disease
IFN: interferon
IL: interleukin
JAK: Janus kinase
JAID: JAK1 associated inflammatory disease
NGS: next generation sequencing
PBMCs: peripheral blood mononuclear cells
STAT: signal transducer and activator of transcription

Introduction:

Cytokines are soluble effector proteins produced by a variety of cells of hematopoietic or stromal origin that act as key regulators of both the innate and the adaptive immune response. As such, a significant number of pathogenic variants of cytokines, receptors to cytokines or proteins involved in downstream signalling, such as proteins of the Janus kinase (JAK)- Signal transducer and activator of transcription (STAT) (JAK-STAT) pathway, have been associated with rare inborn errors of immunity (1). Inborn errors of immunity are heterogeneous rare diseases secondary to monogenic germline pathogenic variants resulting in autoimmunity, autoinflammation, allergy, and increased susceptibility to infectious diseases and/or malignancy (2–4).

Beyond simply increasing our understanding of the immune system, identifying such disorders has an obvious interest in selecting the most appropriate management strategy for patients that often have a long personal history of multiple treatment failures (5,6). Indeed, cytokines, their receptors and members of the JAK/STAT pathway are the targets of an increasing number of innovative treatments developed in recent years that are now used in daily clinical practice (7–9). These drugs, originally developed to treat more common immunological or haematological diseases, are therefore broadly available for prompt and targeted treatment of these rare patients, achieving an efficient translational medicine approach.

Here, we investigated 9 patients of a large French family affected by a dominantly inherited early-onset immune dysregulation syndrome with prominent allergy and autoinflammation related to a previously unreported heterozygous p.Cys787Phe gain of function (GOF) variant of *JAK1* gene**.** JAK1 is involved in the signalling of multiple cytokine receptors including those of the interferon (IFN), gp130, γ_c type, IL-3/β_c and single chain families (10). JAK1 associated inflammatory disease (JAID)(11) is an extremely rare and poorly understood condition previously reported in only 5 individuals from 3 kindreds (12–14). We describe the unique clinical and immunological characteristics associated with the same Cys787Phe pathogenic variant and report the therapeutic efficacy of two JAK inhibitors with a follow-up of 2 years.

Methods

Patients and study approval

All patients, or parents for children, and healthy relatives provided written informed consent for participation, genetic testing, and blood samples. As part of their routine care, patients underwent a series of complete physical examinations and several biological, radiological and pathological studies.

Genetic investigation

We performed a Next Generation Sequencing (NGS) panel targeting 300 genes causal of PID (15). This strategy led to the identification of a heterozygous missense variant in the exon 19 of *JAK1* gene. This *JAK1* variant was confirmed by Sanger sequencing for the index case and several members of his kindred.

Functional Studies

We obtained blood and tissue samples from the study participants to assess the inflammatory profile. Circulating cytokine and allergic related mediator dosages were performed on plasma according to standard procedures. PBMCs or whole blood cells were incubated at 37°C with IFN-α2, IL-2, IL-4 or IL-6 for 30 min. Cellular response was then assessed using fluorescence activated cell sorting (FACS) or mass cytometry (CyTOF). For treated conditions, cells were incubated at 37°C with baricitinib (200 nM) for 15 min prior to cytokine stimulation.

To study the transcriptomic signature of the disease, and the response to baricitinib treatments a total of 100 ng RNA per sample was used to assess the expression of 750 genes involved in immunity with the nCounter Human Autoimmune Profiling Panel (Nanostring).

Additional details are provided in the Supplementary Appendix.

Results

Disease manifestations

From birth, the index patient (V-1) had presented severe dermatitis and multiple food allergies, leading to the identification of a complex immune dysregulation syndrome of apparently dominant inheritance within his family. All affected individuals displayed diffuse ichthyosiform skin lesions and atopic dermatitis-like presentation (Table 1 and S1, Fig. 1 and S1). The ichthyosisform skin lesions were characterized by scaling and hyperkeratosis, with occasional cracks in the palms and erythematous areas. None of the individuals had bullous or erythrodermal lesions as part of the ichthyosis. The skin was also lichenified with areas of intense xerosis and infiltrated erythematous lesions especially on the face in most patients. CT scan in all affected adults identified disseminated nodules of soft tissue density with occasional calcification involving both thoracic and abdominal cavities as well as testis (Fig. 1E). Though most patients did not report symptoms related to the nodules, patient IV-5 underwent orchidectomy due to concerns about possible testicular cancer and developed dysphagia due to a large lower esophageal lesion. Pathological examination of these tumors revealed hypocellular hyalinized collagen with uniform proliferation of fibroblastic spindle cells, inflammatory infiltrate, and large ranges of calcifications, consistent with benign calcifying fibrous tumors (Fig. S2). Besides these common features, patients displayed various other manifestations: oligoarthritis, asthma, susceptibility to warts and ENT infections and chronic diarrhea. Fecal calprotectin, digestive endoscopies with systematic gastrointestinal biopsies were normal except in patient IV-7 in whom exulcerated nodular lesions of the lower esophagus and aphthoid lesions of the jejunum and ileum were found. Biopsies of the ileal lesions showed aspecific inflammation. The diagnosis of unclassified IBD was made in this patient, while the others were diagnosed with motility-related diarrhea. Of note, most patients also had food allergies that started in childhood and improved spontaneously over time. Failure to thrive was noted in two children with severe food allergies and two adults had a short stature. Additionally, two patients displayed unique features: III-6 had a voluminous nodular splenomegaly related to sclerosing angiomatoid nodular transformation (Fig. S2) and IV-5 had Addison's disease.

All patients displayed biological features of allergy: all had extremely high whole blood histamine levels, and most of them displayed mild basophilia, high total IgE levels, and mild eosinophil elevation between 500 and 2000/mm^3. Mild hypogammaglobulinemia was noted in 4 patients. Blood lymphocyte phenotyping revealed inconstant CD3 and CD19 lymphocytosis (Fig. S3). Broad autoimmunity screening was inconclusive (Table S2).

For dermatitis, all patients were treated with emollients and antihistamines, and some also received topical corticosteroids and topical tacrolimus with only moderate relief of symptoms. Patient IV-7 had previously been treated with several lines of immunosuppressants and biologic therapies for IBD/inflammatory rheumatism association (Table S1). Only infliximab led to a partial response of the inflammatory rheumatism, while both digestive and cutaneous involvements remained unchanged. Her father, patient III-6, had previously received adalimumab for oligoarthritis, which had no effect.

Genetic investigations

Next generation sequencing in the proband, his brother and father using a panel for primary immunodeficiencies and revealed the presence of a heterozygous variant: c.2360 G>T; p.(Cys787Phe) in *JAK1* (NM_002227.4). The variant was then confirmed using Sanger sequencing (Fig 2). This variant has not yet been implicated in a pathological condition and is absent from the human gene mutation database. Moreover, this variant was considered private to this family as it was not found in the public gnomAD 2.1.1 database. Subsequent targeted Sanger sequencing of *JAK1* gene in relatives revealed that all the tested affected subjects carried the same variant c.2360G>T in a heterozygous state, while the variant was absent in all the tested healthy siblings (Fig. 2A). The co-segregation of this variant with the clinical phenotype was fully consistent with the autosomal dominant inheritance model of the disease in this family. The variant leads to replacement of an evolutionary highly conserved cysteine and was predicted to be deleterious by all tested models. (Fig 2C). This amino acid is localized in the pseudokinase domain of JAK1, *i.e.* the domain affected by the three previously described GOF *JAK1* pathogenic variants (Fig 2D and S4A). Modelling of the impact of the variant on human JAK1 protein predicted that the phenylalanine residue in position 787 formed new stabilizing interactions with Cys817 and Tyr788 (Fig. 2E).

Patients with JAK1 pseudo kinase domain pathogenic variant Cys787Phe demonstrate altered JAK/STAT signaling.

All tested patients demonstrated an upregulation of the Th1 (IL-12p70, IFNγ) and Th17 (IL-6, IL-12p19, IL-1β) cytokines as well as increased IL-3, IL-33 and TSLP. Th2 cytokines IL-4, IL-13 and IL-10 were significantly lower in the patients compared to healthy donors. (Fig 3A). Nine out of the 10 tested patients returned negative Type I interferon signature (16). III-13 was positive on a first occasion and negative on a second (Fig. S5 A, B, C and D). Targeted transcriptomic analysis of peripheral blood of 4 patients prior to treatment and 4 healthy donors, was performed using a panel of 750 immune genes. Again, no enrichment of a Type I interferon signature was observed. Most enriched pathways concerned over expression of genes related to JAKs/STATs (*JAK1, JAK2, JAK3, STAT3, STAT5b)* signaling (Figs. 3B and 3C). Consistently, immunochemistry analysis on ichtyosiform skin lesions from the patients revealed overexpression of STAT3 and JAK1 (Fig. 3D). Both JAK1 and STAT3 were also highly expressed in calcifying fibrous tumors of JAK1 patients but not in digestive biopsies (Fig. S2A and S2B).

Previoulsy reported *JAK1* pseudokinase domain pathogenic variants led to aberrant STAT activation (12–14). While we noted high STATs activation in whole blood cells from V4, the phosphorylation status of STAT1, STAT3, STAT5 and STAT6 was comparable in the other tested patients to the levels observed in healthy donors for most cell types (Fig 4A, and Fig S6A) and no shared differences were observed across the 5 tested patients. Consistent results were found when studying basal STATs phosphorylation status in frozen PBMC by flow cytometry (Fig S6 B). To study JAK1 hyper and biased activation we stimulated PBMCs from patients with 5 cytokines of which the receptors are known to signal via JAK1: IFNα, IFNγ, IL-2, IL-4 and IL-6 (Fig 4B and Fig S7). Heterogeneous results were observed when comparing the phosphorylation of the canonical STATs for each of these cytokines between patients and controls (IFNα and IFNγ / STAT1, IL-2 / STAT5b, IL-4 / STAT6 and IL-6 / STAT3). Following IFNα stimulation, STAT1 phosphorylation was higher in T cells from III-6, IV-5, IV-9 and II-16 than in T cells from 4 tested healthy donors. The same was true for B cells from patients IV-9 and II-16 and NK cells from patients IV-5, IV-9 and II-16. Similarly, STAT3 phosphorylation was higher in B cells, NK cells and monocytes from patients III-6 following IL-6 stimulation compared to healthy donors. Interestingly, PBMCs of 5 out of the 6 tested patients demonstrated hyper-

phosphorylation of STAT3 in response to stimulation with IFN-α2 (Patients IV-7 and IV-9) or IL-2 (Patients III-6, IV-5 and V-1) when compared to PBMCs from healthy donors. PBMCs from Patients IV-7 and IV-9 also demonstrated hyper-phosphorylation of STAT5b under IFN-α2 stimulation (Fig. 4B). This atypical activation of STAT3 under IL-2 stimulation was confirmed in whole blood (Fig 4C) and appeared to predominantly affect NK cells (both $CD56^{dim}$ and $CD56^{hi}$ populations) (Fig 4C, S8A and S8B). Taken together, our *in vitro* and *ex vivo* experiments reveal a heterogeneous inflammatory profile between patients that converge towards an overexpression and an atypical activation of STAT3 in individuals bearing the $JAK1^{Cys787Phe}$ variant in this kindred.

Patients with *JAK*1 pathogenic variant have an altered basophilic phenotype

All patients displayed extremely high levels of blood histamine level and 6 out of 9 of them had mild basophilia. Comparison with 12 consecutive patients with familial Mediterranean fever, 10 consecutive patients with moderate-to-severe atopic dermatitis and 10 consecutive all-coming patients seen for routine outpatient clinical exams confirmed a significant elevation of basophils in $JAK1^{Cys787Phe}$ patients' blood (Fig. 5A). This basophilic expansion was also observed at the transcriptomic level. Indeed, differential gene expression analysis from peripheral blood of 4 untreated patients compared to healthy donors revealed a basophilic signature defined by the over expression of *IL4, MS4A2*, *HDC* and *CPA3.* (Fig. 5B). Histamine levels was quantified in sorted leukocyte populations from affected individuals and HD showing that basophils contained the largest amount (Fig. 5C). No significant variation in the cellular histamine content between affected individuals and HD including basophils was detected (Fig. 5D). Altogether, this suggests that the high blood histamine levels observed in $JAK1^{Cys787Phe}$ patients mostly results from a mild chronic basophil expansion. In order to test the activation status of circulating basophils we looked at the expression of the following activation markers: CD63, CD69; CD107a, CD193 and CD203c. None of these markers were over expressed on basophils from tested patients compared to healthy donors (Fig 5E).

Treatment with baricitinib

Considering their previously reported efficacy in patients with *JAK1*-pseudokinase domain-GOF variants (12,13), and their indication in atopic dermatitis (17,18), JAK inhibitors were considered for the treatment of our patients. Baricitinib was first tested because of the availability of pharmacokinetic data in children (19). Six adults (II-16, III-4, III-6, III-13, IV-5 and IV-7) and 1 child (V-1) received baricitinib at a dose of 4 and 2 mg once daily respectively. All adults displayed a dramatic skin improvement within a few days following the treatment introduction. Beyond the complete resolution of almost all symptoms related to atopic dermatitis, ichthyosiform lesions gradually improved leading to a drastic reduction in the daily usage of emollient cream and ultimately to a better quality of life (Figs. 6A and 6B and S9). Three out of four patients with chronic diarrhea and two out of three with arthromyalgia experienced substantial improvement of their symptoms. Calcifying fibrous tumors, however, did not regress under baricitinib. V-1, the only treated child, displayed a less positive response with slightly improved ichthyosis and persistent atopic features (Fig. 6B). Moreover, baricitinib did not restore normal ponderal and statural growth.

Inflammatory phenotype modifications with baricitinib treatment were assessed *ex vivo* and *in vitro*. Under baricitinib, all the elevated cytokines decreased except for the V-1 patient. Similarly, IL-4, IL-10 and IL-13 plasmatic levels increased (Fig. 6C , Fig S10 and Table S3). The blood transcriptional analysis under baricitinib treatment revealed a loss of all the previously enriched gene sets related to JAKs/STATs signaling (Fig. S11). *In vitro,* baricitinib achieved a good control of the STAT3 and STAT5b atypical activation following IFN α2 stimulation (Fig. S12). However, STAT3 hyper-phosphorylation following IL-2 stimulation was poorly controlled *in vitro* by the treatment.

Interestingly, despite clinical improvement of atopic features in adults, neither blood histamine levels nor basophilia decreased under baricitinib treatment (Fig. S13A). Accordingly, differential gene expression analysis in whole blood showed a persistent basophilic transcriptional signature (Fig. S13B).

Thus, treatment with baricitinib substantially attenuated the clinical manifestations of the disease and reverted most of the cellular and molecular inflammatory phenotypes driven by $JAK1^{Cys787Phe}$.

Treatment with upadacitinib

Although clinically effective, treatment with baricitinib was not sufficient to fully control all symptoms of the disease. Upadacitinib, a specific JAK1 inhibitor, was tested in 4 adult patients (III-4, III-6, IV-5 and IV-7) and was able to control canonical STAT1 and STAT5 activation following IFNα and IL-2 stimulation of patients' whole blood (Fig S14). Cutaneous and articular involvements worsened in 3 (III-6, IV-7 and III-4) and 2 (IV-7 and III-4) patients respectively. Two patients who displayed persistent gastrointestinal manifestations under baricitinib (III-6 and IV-7) experienced a substantial reduction of stool frequency and abundance with upadacitinib. (Fig. S15) Overall, due to the dissociated response under upadacitinib, patients III-6, IV-7 and III-4 were switched back to baricitinib; while only patient IV-5 remained under upadacitinib. He displayed an overall diminution of most inflammatory cytokine levels under upadacitinib compared to baricitinib (Fig S16). After resuming treatment with baricitinib, cutaneous (III-6, IV-7 and III-4) and articular (IV-7 and III-4) symptoms improved again.

Discussion

We report a large French family displaying a complex immune dysregulation syndrome with predominant cutaneous involvements perfectly segregating with the heterozygous *JAK1*: p.Cys787Phe variant. The main features, mostly related to atopy and/or autoinflammation, are close to what has been reported in the previously described *JAK1* pathogenic variants (12–14). This large family with this novel *JAK1* pathogenic variant harbors some specific features such as diffuse ichthyosiform skin rash, very high blood histamine levels associated with mild basophilia and multiple profound benign calcified tumours. These clinical and biological specificities are simple to identify on clinical examination or through blood sampling and could constitute markers indicative of JAK1-associated inflammatory disease (JAID) for the clinician. As a result, we expect them to be valuable in guiding the clinical diagnosis of a JAID among patients with familial atopic dermatitis/ichthyosis.

Our observation highlights that the clinical heterogeneity reported in patients with *JAK1* GOF variants is mirrored by a variable dysregulation of the JAK/STAT signalling pathway. Indeed, despite careful assessment using three different assays, and in contrast to the patient with the S703I mosaic, we did not observe any consistent type I IFN signature in our family. This is reminiscent of what is observed in STAT1 GOF variants, in which type I interferon signature is

variably present across patients or variants (20). Increase of the constitutive basal activation of the JAK/STAT signalling pathway was variable across patients. Cytokine-induced hyperphosphorylation of canonical JAK/STAT pathways was variably observed across patients, in opposition to previous report on patients with A634D and 703I *JAK1* GOF variants (12,13). This discrepancy might be partly explained by the larger group of patients and controls (heathy donors) used in our study compared to the previous reports, better encompassing the inter-individual variability of both control and patient groups. Together, our observation of JAK/STAT signalling in our patients imply that lack of type I interferon signature and more generally lack of over activation of canonical JAK/STAT pathway should not be considered as excluding criteria for *JAK 1* GOF diagnosis.

Besides this clinical and molecular heterogeneity, there are compelling associations pointing toward a common pathophysiology. The first are the above-mentioned shared clinical features, which mainly consist in atopic manifestations such as atopic dermatitis, food allergy, asthma, and eosinophilia (Fig. S17). The second is the existence of common dysregulations of the STATs phosphorylation by JAKs in patients with a *JAK1* GOF variant. Indeed, as for *JAK1* S703I mosaic variant, we observed a consistent atypical phosphorylation of STAT3 and STAT5b in cells from patients with the Cys787Phe pathogenic variant. This finding is highly consistent with the phenotypic overlap of JAK1 associated disease with manifestations observed in patients with *STAT3* and *STAT5b* GOF pathogenic variants (21,22) (Table 2).

It might be important however to highlight that we observed a trend toward hyperphosphorylation of STAT6 following IL-4 treatment. Given the clinical overlap of STAT6 GOF (23–25) patients with JAK1 GOF patients (Table2), it is reasonable to speculate that hyperphosphorylation of STAT6 might contribute to the allergic manifestation in JAK1 GOF patients.

Baricitinib treatment resulted in a major improvement of most of atopic and inflammatory manifestations among adults, especially ichthyosis-related and atopic dermatitis-related symptom, achieving a substantial improvement of quality of life. This good clinical response was consistent with the partial correction or normalization of all dysregulated cytokines and the extinction of the JAKs/STATs signaling transcriptomic signatures. However, in some patients, treatment with baricitinib was not sufficient to fully control digestive and articular features leading us to switch to upadacitinib, a selective JAK1 inhibitor, in 4 patients. Digestive manifestations improved (n=2), however skin and/or articular involvements worsened (n=3).

As suggested *in vitro* (13), our results support that selective JAK1 inhibition might not be an optimal therapeutic approach in patients with *JAK1* associated disease. Indeed, it remains unclear how a variant in the JAK1 pseudokinase domain could lead to atypical STAT3 and STAT5b activation. To date, the function of JAK1 pseudokinase domain in the overall protein function, including regulation of the catalytic activity or binding/recruitment of signalling partners, remains largely unknown (26). Disease-causing variants of the *JAK1* pseudokinase domain could favour JAK2 trans-activation. This hypothesis is partly supported by our observations that in most patients the disease was better controlled by the JAK1/JAK2 inhibitor baricitinib than by the selective JAK1 inhibitor upadacitinib.

Interestingly, AD was a common feature of our patients, suggesting that JAK1 dysregulation might account for some common forms of AD. The spectacular efficacy of baricitinib on our patients' dermatitis suggest that a proportion of AD patients with altered JAK1 signalling would have particularly high benefit from this therapy.

Despite the above-mentioned efficacy of JAKinibs to treat skin atopic manifestations, both baricitinib and upadacitinib failed to control the basophilic signature of the disease, suggesting a pathway independent of JAK1/2 kinase activity might drive this basophilia. Thus, the precise basophil contribution to the disease pathogenesis is not yet elucidated. One child received baricitinib resulting in decreased pruritus and better sleep without improvement of his food allergy. The treatment improved the skin involvement. However, considering the potential risk on growth due to blocking of growth hormone signalling, baricitinib was discontinued.

The description of this large family with inherited JAID expends the clinical spectrum of the disease and can guide the future diagnosis of such patients. Two years follow-up of our patients under baricitinib treatment reveals a clear benefit of JAK1 and JAK2 inhibition for the control of most disease manifestation. Finally, the clinical response to various JAK inhibitor treatment regimens of JAID patients provides useful information on their benefits among patients suffering from more common diseases such as atopic dermatitis, chronic inflammatory rheumatism, or inflammatory bowel diseases.

Authors contributions

MPR and SGL conceived and designed the study. AF, MPR and SGL wrote the paper. VH and JML contributed to writing the paper. AF, CPo, AC, CLL, JLC, SD, MF, BH, PM, MP, JML, JC, NS, YYJZ, SM and MPR performed experiments, AF, CPo, AC, CLL, MC, MM, SD, MF, LLC, TRJM, PM, CPi, SV, DD, JML, JC, JPH, MPR, NS, YYJZ, SM, AH, RRB, TTM and SGL performed data analysis. AF, VH, CL, JDK, VL, TM, MHS, SGL were involved in the clinical study and sample collection. All authors reviewed the manuscript and gave final approval for the version to be published. All authors agree to be accountable for all aspects of the work in ensuring that questions related to the accuracy or integrity of any part of the work are appropriately investigated and resolved.

Acknowedgments

We thank all the affected patients and their family, and the healthy individuals used as controls, researchers from Inserm UMRS_933 laboratory for helping with the identification of the mutation, Mr Benjamin SaintPierre and Ms Lucie Adoux from the Genomic platform of Cochin Institute for their precious help in producing/analysing the data, the CBUtechS platform of the Institut Pasteur for supporting generation of Nanostring data, Dr. Lauriane Goldwirt for performing baricitinib blood assay in treated patients, the cyto2BM core facility of BioMedTech Facilities INSERM US36 | CNRS UAR20 for helping with flow cytometry experiment ~~and~~ , the Agence Régional de Santé Île-de-France and les hôpitaux universitaires de Strasbourg for supporting the project with the “bourse année-recherche” educational grant and “la Fondation pour la Recherche Medical” for providing the Ph.D scholarship of Margaux Cescato.

Competing interests : none

Funders

SGL: ANR INFLAMAST AAPG 2017 CE17 and foundation APHP.
MPR was supported by the Agence National de la Recherche: ANR-21-CE17-0025 JDMINF2.

Data Availability

The datasets generated during and/or analysed during the current study are available from the corresponding author on reasonable request.

Bibliography

1. Boisson B, Quartier P, Casanova J-L. Immunological loss-of-function due to genetic gain-of-function in humans: autosomal dominance of the third kind. Curr Opin Immunol. 2015 Feb;32:90–105.
2. Notarangelo LD, Bacchetta R, Casanova J-L, Su HC. Human inborn errors of immunity: An expanding universe. Sci Immunol. 2020 Jul 10;5(49).
3. Tangye SG, Al-Herz W, Bousfiha A, Chatila T, Cunningham-Rundles C, Etzioni A, et al. Human Inborn Errors of Immunity: 2019 Update on the Classification from the International Union of Immunological Societies Expert Committee. J Clin Immunol. 2020 Jan 17;40(1):24–64.
4. Tangye SG, Al-Herz W, Bousfiha A, Cunningham-Rundles C, Franco JL, Holland SM, et al. The Ever-Increasing Array of Novel Inborn Errors of Immunity: an Interim Update by the IUIS Committee. J Clin Immunol. 2021 Feb 18;
5. Hadjadj J, Frémond M-L, Neven B. Emerging place of JAK inhibitors in the treatment of inborn errors of immunity. Front Immunol. 2021 Sep 17;12:717388.
6. Lin B, Goldbach-Mansky R. Pathogenic insights from genetic causes of autoinflammatory inflammasomopathies and interferonopathies. J Allergy Clin Immunol. 2021 Dec 7;
7. Lamb CA, Kennedy NA, Raine T, Hendy PA, Smith PJ, Limdi JK, et al. British Society of Gastroenterology consensus guidelines on the management of inflammatory bowel disease in adults. Gut. 2019 Dec;68(Suppl 3):s1–s106.
8. Fraenkel L, Bathon JM, England BR, St Clair EW, Arayssi T, Carandang K, et al. 2021 american college of rheumatology guideline for the treatment of rheumatoid arthritis. Arthritis Care Res (Hoboken). 2021 Jul;73(7):924–939.
9. Chovatiya R, Paller AS. JAK inhibitors in the treatment of atopic dermatitis. J Allergy Clin Immunol. 2021 Oct;148(4):927–940.
10. Morris R, Kershaw NJ, Babon JJ. The molecular details of cytokine signaling via the JAK/STAT pathway. Protein Sci. 2018 Dec;27(12):1984–2009.
11. Biggs CM, Cordeiro-Santanach A, Prykhozhij SV, Deveau AP, Lin Y, Del Bel KL, et al. Human JAK1 gain of function causes dysregulated myelopoeisis and severe allergic inflammation. JCI Insight. 2022 Dec 22;7(24).
12. Del Bel KL, Ragotte RJ, Saferali A, Lee S, Vercauteren SM, Mostafavi SA, et al. JAK1 gain-of-function causes an autosomal dominant immune dysregulatory and hypereosinophilic syndrome. J Allergy Clin Immunol. 2017 Jun;139(6):2016–2020.e5.
13. Gruber CN, Calis JJA, Buta S, Evrony G, Martin JC, Uhl SA, et al. Complex autoinflammatory syndrome unveils fundamental principles of JAK1 kinase transcriptional and biochemical function. Immunity. 2020 Sep 15;53(3):672–684.e11.
14. Takeichi T, Lee JYW, Okuno Y, Miyasaka Y, Murase Y. Autoinflammatory keratinization disease with hepatitis and autism reveals roles for JAK1 kinase hyperactivity in autoinflammation. Frontiers in Immunology. 2021;12:737747
15. Fusaro M, Rosain J, Grandin V, Lambert N, Hanein S, Fourrage C, et al. Improving the diagnostic efficiency of primary immunodeficiencies with targeted next-generation sequencing. J Allergy Clin Immunol. 2021 Feb;147(2):734–737.
16. Rice GI, Forte GMA, Szynkiewicz M, Chase DS, Aeby A, Abdel-Hamid MS, et al. Assessment of interferon-related biomarkers in Aicardi-Goutières syndrome associated

with mutations in TREX1, RNASEH2A, RNASEH2B, RNASEH2C, SAMHD1, and ADAR: a case-control study. Lancet Neurol. 2013 Dec;12(12):1159–1169.
17. He H, Guttman-Yassky E. JAK inhibitors for atopic dermatitis: an update. Am J Clin Dermatol. 2019 Apr;20(2):181–192.
18. Guttman-Yassky E, Silverberg JI, Nemoto O, Forman SB, Wilke A, Prescilla R, et al. Baricitinib in adult patients with moderate-to-severe atopic dermatitis: A phase 2 parallel, double-blinded, randomized placebo-controlled multiple-dose study. J Am Acad Dermatol. 2019 Apr;80(4):913–921.e9.
19. Kim H, Brooks KM, Tang CC, Wakim P, Blake M, Brooks SR, et al. Pharmacokinetics, pharmacodynamics, and proposed dosing of the oral JAK1 and JAK2 inhibitor baricitinib in pediatric and young adult CANDLE and SAVI patients. Clin Pharmacol Ther. 2018 Aug;104(2):364–373.
20. Scott O, Lindsay K, Erwood S, Mollica A, Roifman CM, Cohn RD, et al. STAT1 gain-of-function heterozygous cell models reveal diverse interferon-signature gene transcriptional responses. NPJ Genom Med. 2021 May 14;6(1):34.
21. Flanagan SE, Haapaniemi E, Russell MA, Caswell R, Allen HL, De Franco E, et al. Activating germline mutations in STAT3 cause early-onset multi-organ autoimmune disease. Nat Genet. 2014 Aug;46(8):812–814.
22. Ma CA, Xi L, Cauff B, DeZure A, Freeman AF, Hambleton S, et al. Somatic STAT5b gain-of-function mutations in early onset nonclonal eosinophilia, urticaria, dermatitis, and diarrhea. Blood. 2017 Feb 2;129(5):650–653.
23. Sharma M, Leung D, Momenilandi M, Jones LCW, Pacillo L, James AE, et al. Human germline heterozygous gain-of-function STAT6 variants cause severe allergic disease. J Exp Med. 2023 May 1;220(5).
24. Takeuchi I, Yanagi K, Takada S, Uchiyama T, Igarashi A, Motomura K, et al. STAT6 gain-of-function variant exacerbates multiple allergic symptoms. J Allergy Clin Immunol. 2022 Dec 17;
25. Baris S, Benamar M, Chen Q, Catak MC, Martínez-Blanco M, Wang M, et al. Severe allergic dysregulation due to A gain of function mutation in the transcription factor STAT6. J Allergy Clin Immunol. 2023 Feb 7;
26. Raivola J, Haikarainen T, Silvennoinen O. Characterization of JAK1 pseudokinase domain in cytokine signaling. Cancers (Basel). 2019 Dec 27;12(1).

Figure 1: Clinical findings.

A: Bilateral cheek involvement of severe atopic dermatitis-like inflammatory skin lesions in patient V-1. **B:** Inflammatory Linear Verrucous Papules of the forearm in patient IV-5. **C:** Extensive ichthyosiform skin lesions of the breast and forearm in patient II-16. **D:** Digital recurrent warts in patient IV-7. **E:** Sagittal reconstruction of patient IV-5 CT-scan showing multiple calcified nodules of both thoracic and abdominal cavities, including a voluminous lesion of the lower esophagus responsible for dysphagia

Figure 2: Variant in JAK1 pseudokinase domain.

A: Pedigree of the family. Solid symbols indicate affected individuals, open symbols: unaffected individuals, asterisk: genotyped individuals, arrow: proband, slashes: deceased individuals. Non-genotyped individuals were considered to be affected if they displayed early onset dermatitis. JAK1-Cys787Phe variant was found in all tested symptomatic individuals and in none of the clinically asymptomatic relatives. B: Electropherogram of patient V-1 and healthy relative IV-11. C: Alignment of JAK1 homologs illustrates the strict evolutionary conservation of the Cysteine in position 787. D: Representation of the JAK1 domains with localizations of known inflammatory disease-causing variants of the pseudokinase domain. E: Prediction of the impact of the variant on the interactions between the residue in position 787 and other residues.

Figure 3: Patients demonstrate systemic and local inflammation.

A) Representation of the plasmatic concentration of various cytokines in the plasma of healthy donors and JAK1 patients. Results are presented as log2 fold change normalized on the mean of the healthy donors. B) Significantly enriched pathways in patients compared to healthy donors identified by gene set enrichment analysis from transcriptomic study on whole blood. C) Detail of the genes from the identified pathways. D) JAK1 and STAT3 immunostaining of a normal skin biopsy from a healthy donor and an ichthyous skin biopsy from patient III-13

(magnification x400). JAK1 cytoplasmic overexpression of the entire epidermis and STAT3 nuclear overexpression of the upper part of the epidermis were observed in the patient's skin.

Figure 4: Dysregulated phosphorylation of STAT3 in patient's cells.

A)**.** Bar graph showing the phosphorylation of STAT3 in unstimulated fresh whole blood from 4 donors and 5 untreated patients. For IV-7 : Baricitinib discontinuation >72h. B) Phosphorylation status of STAT1, STAT3, STAT5b and STAT6 was measured by flow cytometry on frozen PBMCs from 4 healthy donors and 6 patients stimulated with IFN-α2 (100 UI/mL) and IL-2 (50 ng/mL) C) STAT3 phosphorylation in response to IL-2 assessed by mass cytometry in blood leukocyte subsets from 3 healthy donors (left) and patient IV-7 (right). Each solid circle indicates a cluster. Circle diameter indicates cluster's relative frequency in the sample(s). The continuous color scale depicts the fold change of pSTAT3 mean signal intensity after IL-2 stimulation, compared to baseline pSTAT3 signal intensity assessed in non-stimulated conditions.

Figure 5: Moderate basophilia in JAK1^{C787F} patients.

A) Quantification of circulating basophils in 7 JAK1^{C787F} patients, 10 patients with atopic dermatitis (AD), 12 patients with familial Mediterranean fever (FMF) and 10 consecutive all-coming patients. B) Volcano plot representation of the gene expression analysis comparing patients to healthy donors. *IL4*, a cytokine gene known to be largely expressed in basophils, and 3 of the 4 basophilic genes included in the transcriptomic panel (*MS4A2*, *HDC* and *CPA3*) were among the 7 top upregulated genes in JAK1-Cys787Phe patients. C) Intracellular histamine quantification in circulating leukocyte subsets from patients and healthy donors. D) Intracellular histamine quantification in circulating basophils from patients and healthy donors. E) Evaluation by flow cytometry of the expression of activation markers by basophils from patients and healthy donors.

Figure 6: Response to baricitinib.

A) Three key cutaneous manifestations from two patients are presented before (top) and during treatment with baricitinib (bottom). From left to right: improvement of atopic dermatitis-like lesions of the face in patient III-4 (I); improvement of the inflammatory linear verrucous papules of patient IV-5's forearm (II); and near disappearance of xerosis and lichenification of icthyosiform atopic dermatitis lesions on patient III-4's hand (III). **B)** Effect of baricitinib on the articular, gastrointestinal, and skin involvements using a subjective clinical scale ranging from 0 (no activity) to 5 (severe involvement). **C)** Plasmatic concentration of cytokines in patients before and under treatment with baricitinib. All patients had a partial or total improvement of cytokine levels except V-1.

Table 1:

Summary of the manifestations of the JAK1-associated autoinflammatory disease in this family.

ENT: ear-nose-throat

* all adult patients, children did not undergo systematic CT scans

	Main features	Frequency no./total no
Allergy	Ichthyosis	9/9
	Atopic dermatitis	9/9
	Elevated blood histamine level	9/9
	Moderate basophilia	6/9
	Moderate eosinophilia	5/9
	High total IgE	5/9
Inflammation	Arthralgia	6/9
	Mild inflammatory syndrome	7/9
Immune deficiency	Recurrent ENT infections	5/9
	Susceptibility to warts	4/9
	Mild hypogammaglobulinemia	~~5~~ 4/9
Other	Calcifying fibrous tumors	7/7*
	Diarrhea	5/9
	Short stature / failure to thrive	5/9

Table 2

		JAK1-Cys787Phe	STAT3 AD GOF[$]	STAT5b AD GOF [£*]	STAT6 AD GOF[€]	JAK3 AD GOF[&]
Onset		Neonatal	Childhood	Neonatal	Early chilhood	?
Failure to thrive / short stature		+	+	+	+	?
Atopy	**Atopic dermatitis**	+	+	+	+	-
	Food allergies	+	-	+	+	-
	Asthma	+	-	+	+	-
	Eosinophil count	Moderately elevated	Normal	High	High	-
	Eosinophilic GI disease	-	-	+	+	-
	Basophilia	+	-	-	-	-
	Hyper-IgE	+	-	+	+	-
Auto-immunity / inflammation	**Enteropathy / IBD**	+/-	+	-	-	-
	Arthritis	+	+	-	-	-
	Autoimmune cytopenia	-	+	-	-	+
	Interstitial lung disease	-	+	-	-	-
	Endocrinopathies	Addison's disease	T1D, thyroiditis	-	-	-
Imm. def.	**Hypogammaglobulinemia**	+/-	+/-	-	+/-	+
	Infection susceptibility	Mild	+	-	+	+
	Warts	+	-	-	-	-
Onco-hemato.	**Lymphadenopathy**	+/-	+	-	-	+
	Hepatosplenomegaly	-	+	-	-	+
	Multiple CFT	+	-	-	-	-
	Risk of malignancy	?	+	?	?	?
Other feature(s)		Ichthyosis, CFT, Diarrhea of uncertain cause	-	-	-	CLPD-NK

T1D: Type-1 diabetes melitus; Imm. def.: immune deficiency; CFT: calcifying fibrous tumors; onco-hemato.: onco-hematological features.
GI:gastro intestinal; IBD : intestinal bowel disease
$: adapted from Fabre *et al. J Allergy Clin Immunol Pract* 2019
£: adapted from Ma *et al. Blood* 2017 ; *: somatic mutation
€: adapted from Sharma *et al. J Exp Med* 2023
&: adapted from Lesmana *et al.* Blood 2020

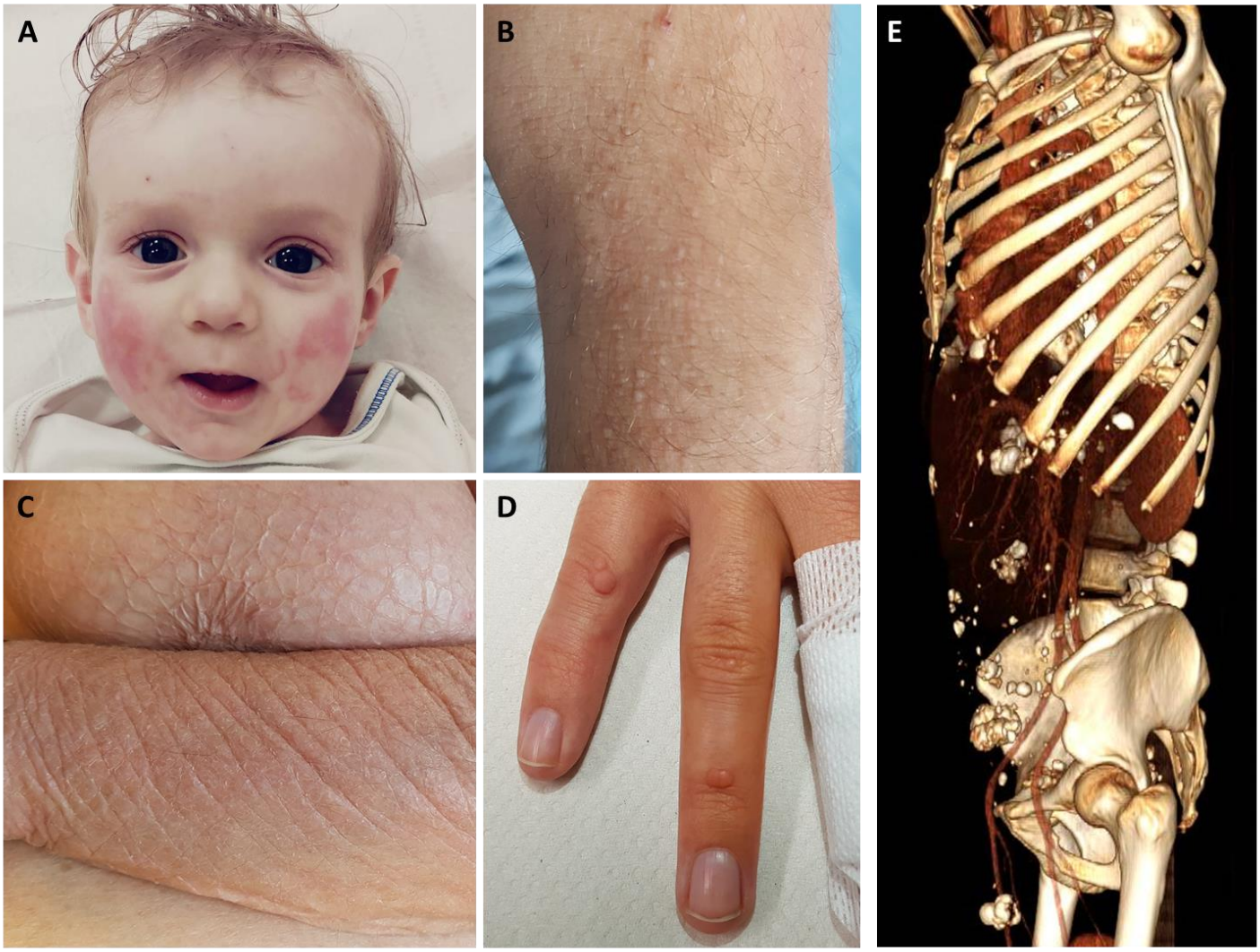
A
B
E
C
D

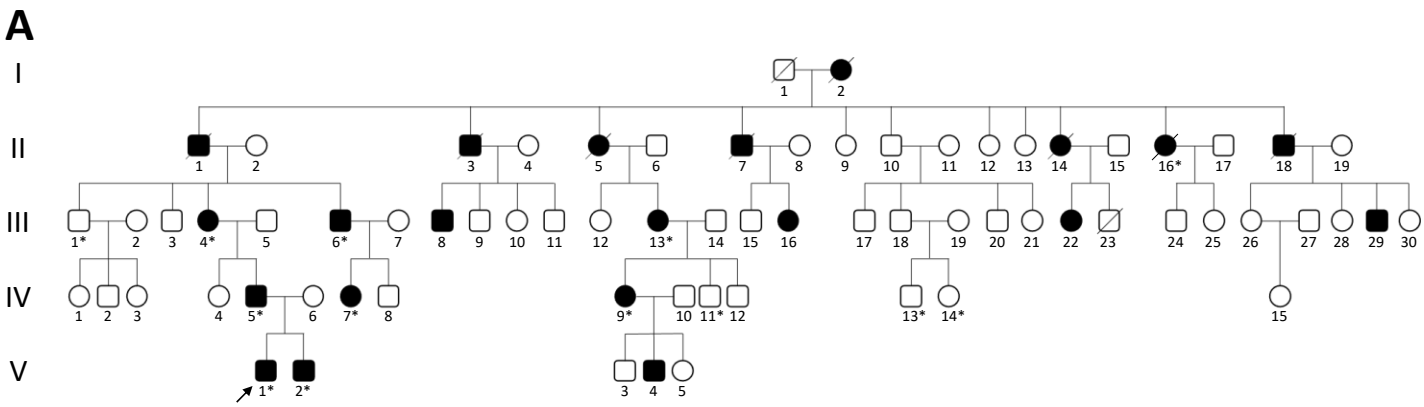
A
I
II
III
IV
V

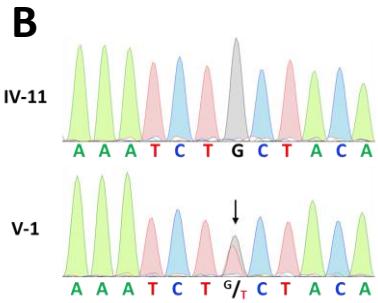
B
IV-11
A A A T C T G C T A C A
V-1
A A A T C T G/T C T A C A

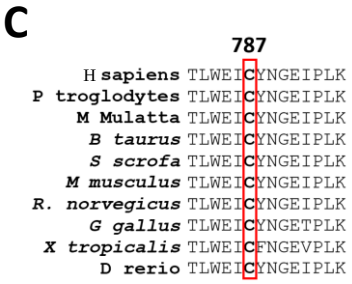
C
787
H sapiens TLWEICYNGEIPLK
P troglodytes TLWEICYNGEIPLK
M Mulatta TLWEICYNGEIPLK
B taurus TLWEICYNGEIPLK
S scrofa TLWEICYNGEIPLK
M musculus TLWEICYNGEIPLK
R. norvegicus TLWEICYNGEIPLK
G gallus TLWEICYNGETPLK
X tropicalis TLWEICFNGEVPLK
D rerio TLWEICYNGEIPLK

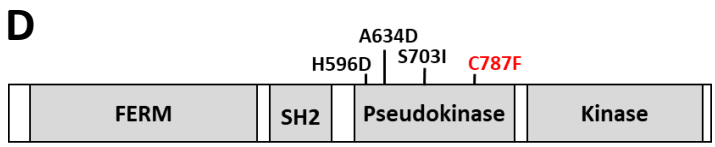
D
A634D
H596D
S703I
C787F
FERM
SH2
Pseudokinase
Kinase

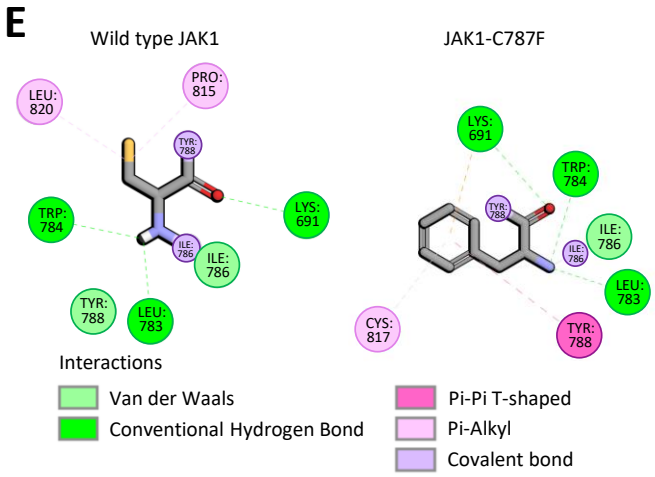
E
Wild type JAK1
JAK1-C787F
LEU: 820
PRO: 815
TYR: 788
LYS: 691
TRP: 784
ILE: 786
TYR: 788
LEU: 783
LYS: 691
TRP: 784
ILE: 786
LEU: 783
CYS: 817
TYR: 788
Interactions
Van der Waals
Conventional Hydrogen Bond
Pi-Pi T-shaped
Pi-Alkyl
Covalent bond

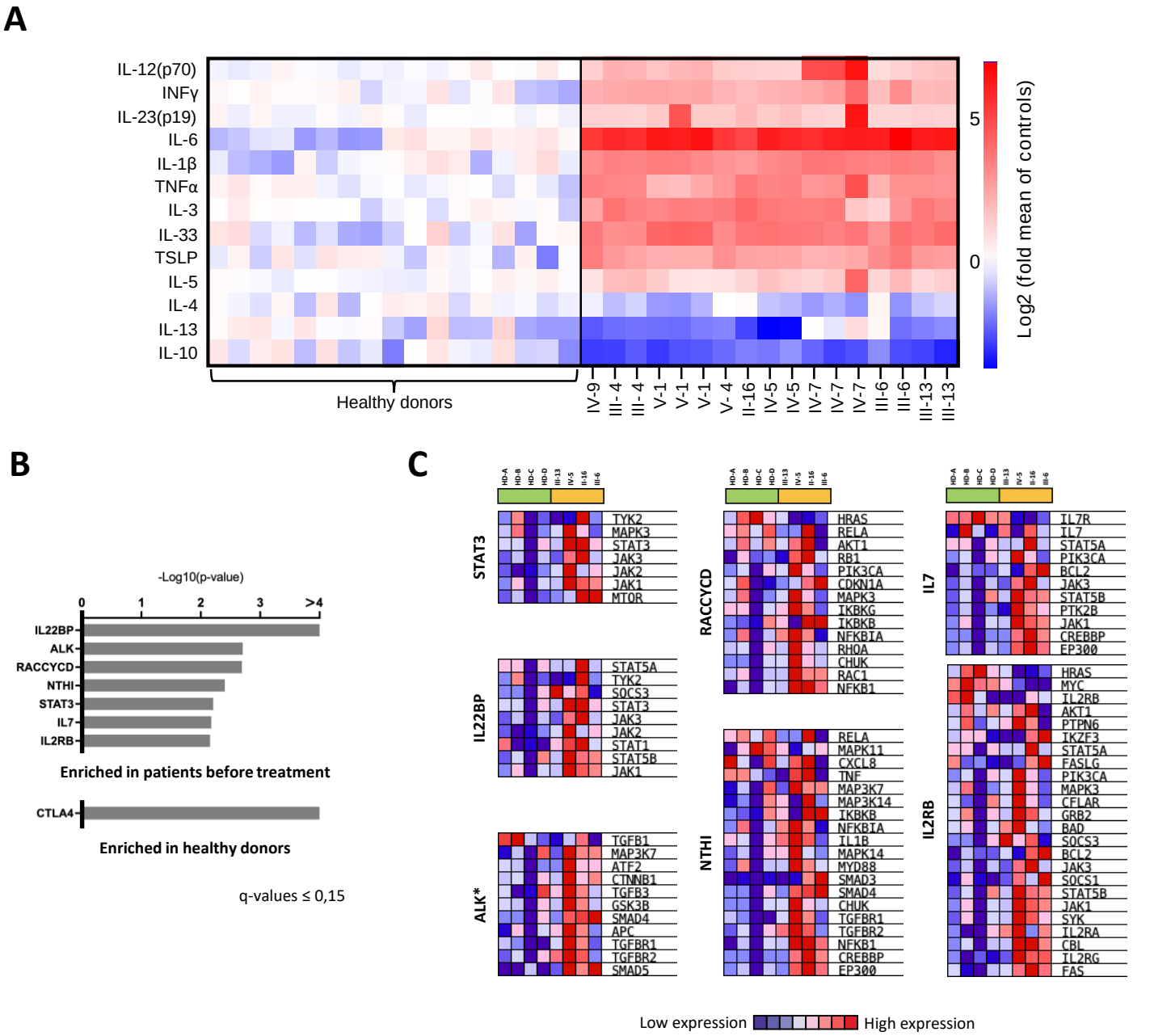
A
IL-12(p70)
INFγ
IL-23(p19)
IL-6
IL-1β
TNFα
IL-3
IL-33
TSLP
IL-5
IL-4
IL-13
IL-10
Healthy donors
IV-9
III- 4
III- 4
V-1
V-1
V-1
V- 4
II-16
IV-5
IV-5
IV-7
IV-7
IV-7
III-6
III-6
III-13
III-13
5
0
Log2 (fold mean of controls)
B
-Log10(p-value)
0
1
2
3
>4
IL22BP
ALK
RACCYCD
NTHI
STAT3
IL7
IL2RB
Enriched in patients before treatment
CTLA4
Enriched in healthy donors
q-values ≤ 0,15
C
STAT3
TYK2
MAPK3
STAT3
JAK3
JAK2
JAK1
MTOR
IL22BP
STAT5A
TYK2
SOCS3
STAT3
JAK3
JAK2
STAT1
STAT5B
JAK1
ALK*
TGFB1
MAP3K7
ATF2
CTNNB1
TGFB3
GSK3B
SMAD4
APC
TGFBR1
TGFBR2
SMAD5
RACCYCD
HRAS
RELA
AKT1
RB1
PIK3CA
CDKN1A
MAPK3
IKBKG
IKBKB
NFKBIA
RHOA
CHUK
RAC1
NFKB1
NTHI
RELA
MAPK11
CXCL8
TNF
MAP3K7
MAP3K14
IKBKB
NFKBIA
IL1B
MAPK14
MYD88
SMAD3
SMAD4
CHUK
TGFBR1
TGFBR2
NFKB1
CREBBP
EP300
IL7
IL7R
IL7
STAT5A
PIK3CA
BCL2
JAK3
STAT5B
PTK2B
JAK1
CREBBP
EP300
IL2RB
HRAS
MYC
IL2RB
AKT1
PTPN6
IKZF3
STAT5A
FASLG
PIK3CA
MAPK3
CFLAR
GRB2
BAD
SOCS3
BCL2
JAK3
SOCS1
STAT5B
JAK1
SYK
IL2RA
CBL
IL2RG
FAS
Low expression
High expression
D
Anti-JAK1
Anti-STAT3
Healthy donor
Patient III-13
Healthy donor
Patient III-13

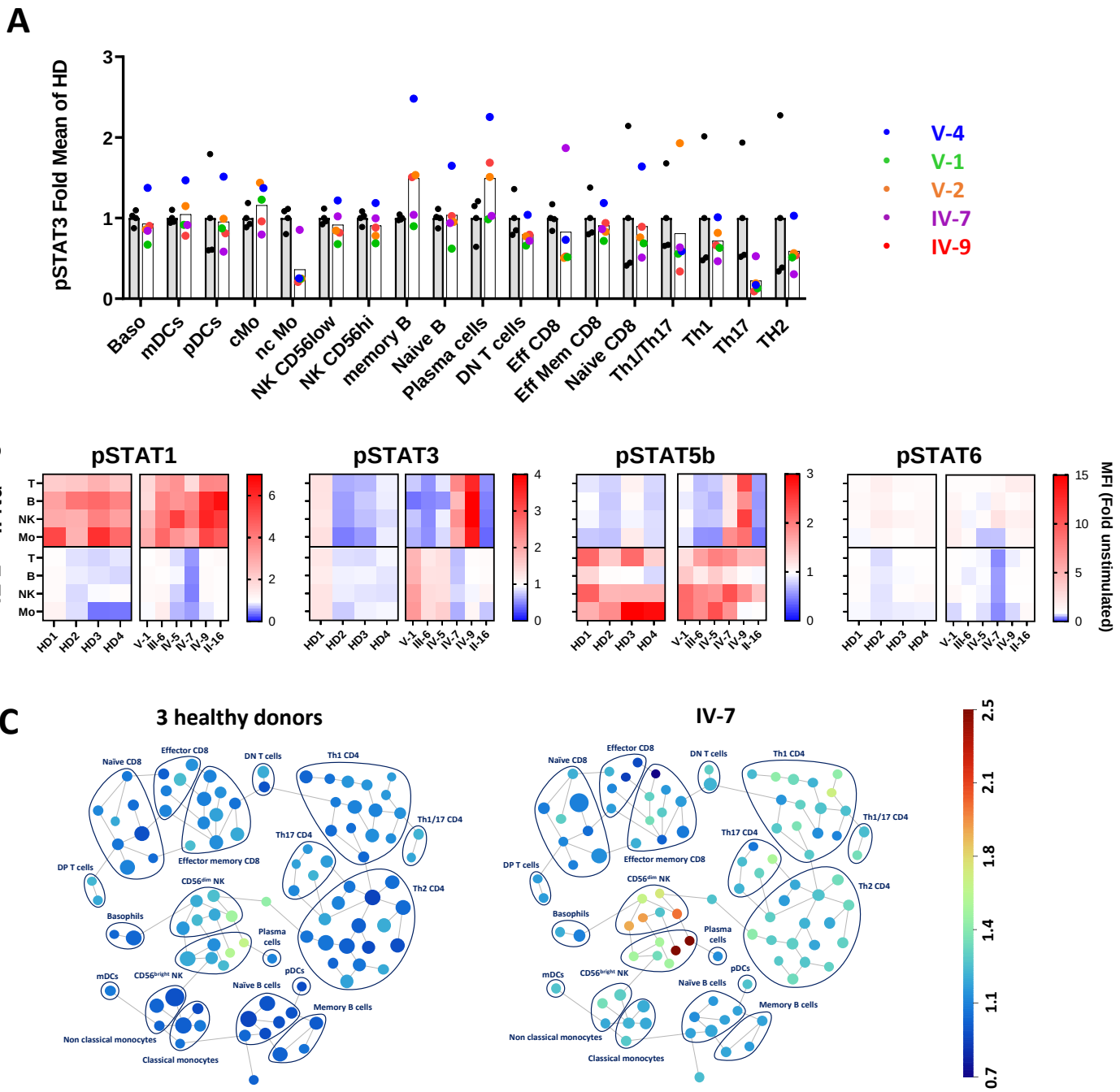
A
pSTAT3 Fold Mean of HD
3
2
1
0
Baso
mDCs
pDCs
cMo
nc Mo
NK CD56low
NK CD56hi
memory B
Naive B
Plasma cells
DN T cells
Eff CD8
Eff Mem CD8
Naive CD8
Th1/Th17
Th1
Th17
TH2
V-4
V-1
V-2
IV-7
IV-9
B
pSTAT1
pSTAT3
pSTAT5b
pSTAT6
IFNα
IL-2
T
B
NK
Mo
HD1
HD2
HD3
HD4
V-1
Ill-6
IV-5
IV-7
IV-9
Il-16
MFI (Fold unstimulated)
C
3 healthy donors
IV-7
Naïve CD8
Effector CD8
DN T cells
Th1 CD4
Th1/17 CD4
Th17 CD4
Th2 CD4
Effector memory CD8
DP T cells
CD56dim NK
Basophils
Plasma cells
pDCs
mDCs
CD56bright NK
Naïve B cells
Memory B cells
Non classical monocytes
Classical monocytes
2.5
2.1
1.8
1.4
1.1
0.7

Figure 5

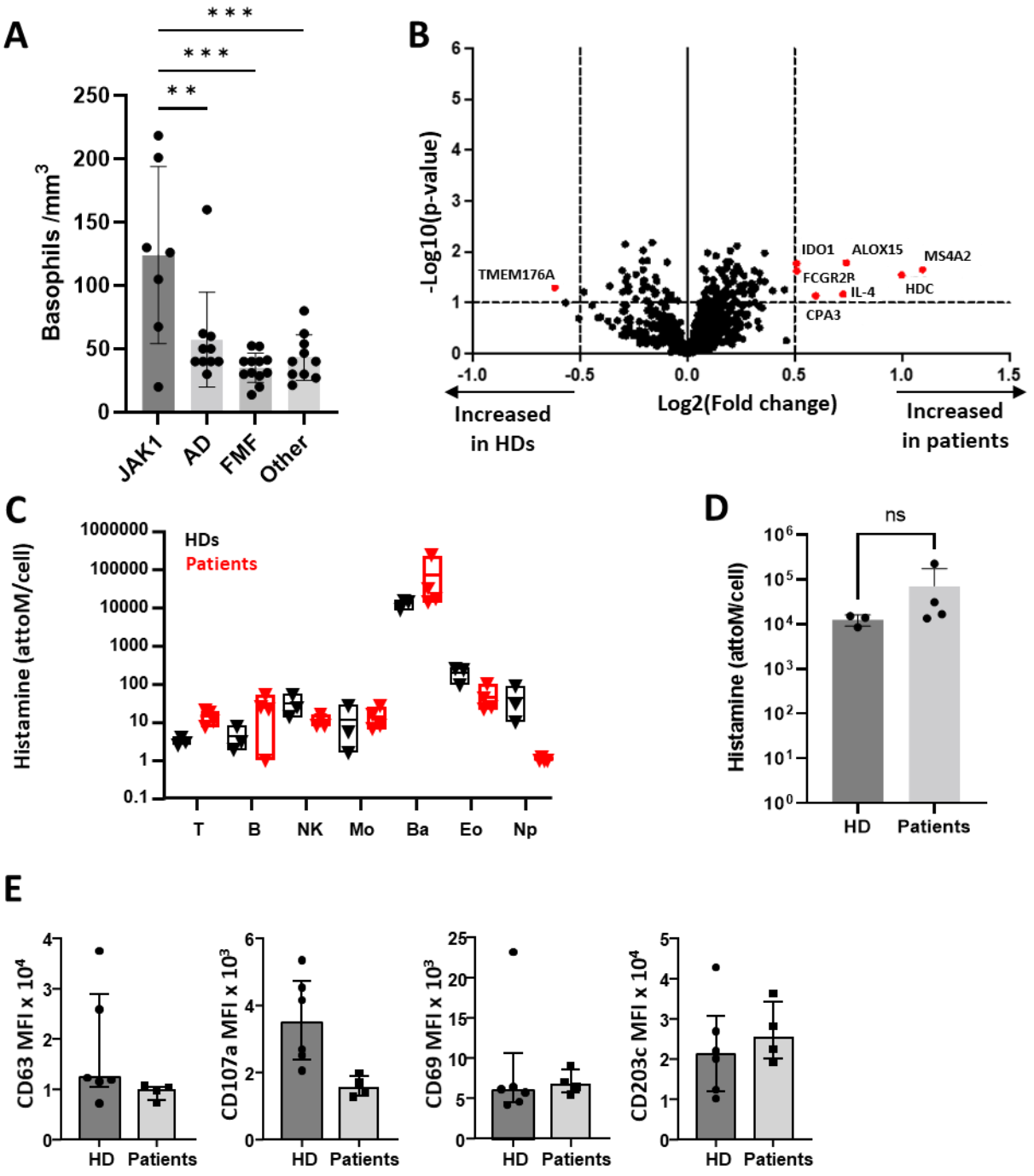
A
***
***
**
Basophils /mm3
250
200
150
100
50
0
JAK1
AD
FMF
Other
B
-Log10(p-value)
6
5
4
3
2
1
0
TMEM176A
IDO1
ALOX15
MS4A2
FCGR2R
IL-4
HDC
CPA3
-1.0
-0.5
0.0
0.5
1.0
1.5
Log2(Fold change)
Increased in HDs
Increased in patients
C
Histamine (attoM/cell)
1000000
100000
10000
1000
100
10
1
0.1
HDs
Patients
T
B
NK
Mo
Ba
Eo
Np
D
Histamine (attoM/cell)
ns
HD
Patients
E
CD63 MFI x 10^4
CD107a MFI x 10^3
CD69 MFI x 10^3
CD203c MFI x 10^4
HD
Patients

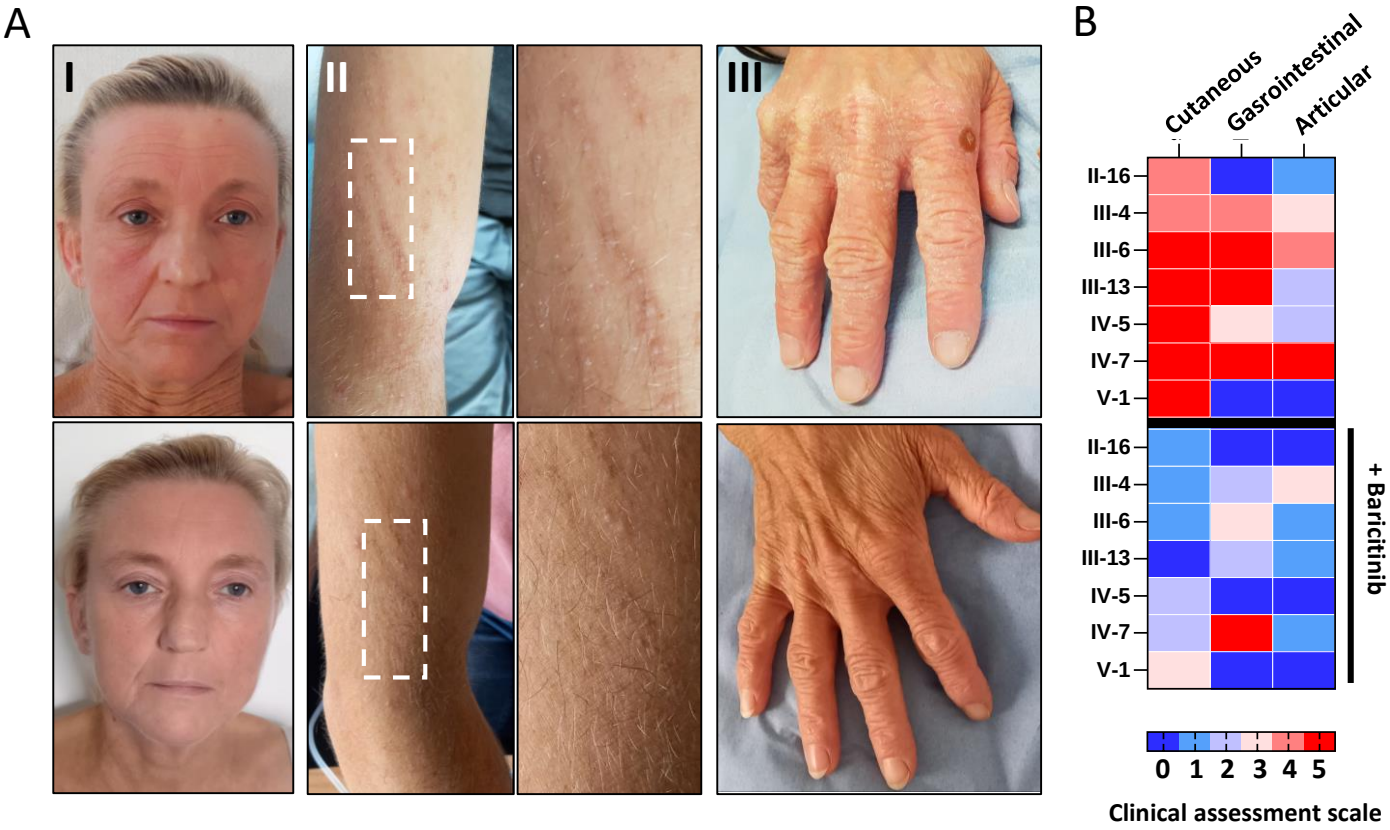
A
I
II
III
B
Cutaneous
Gasrointestinal
Articular
II-16
III-4
III-6
III-13
IV-5
IV-7
V-1
II-16
III-4
III-6
III-13
IV-5
IV-7
V-1
+ Baricitinib
0 1 2 3 4 5
Clinical assessment scale

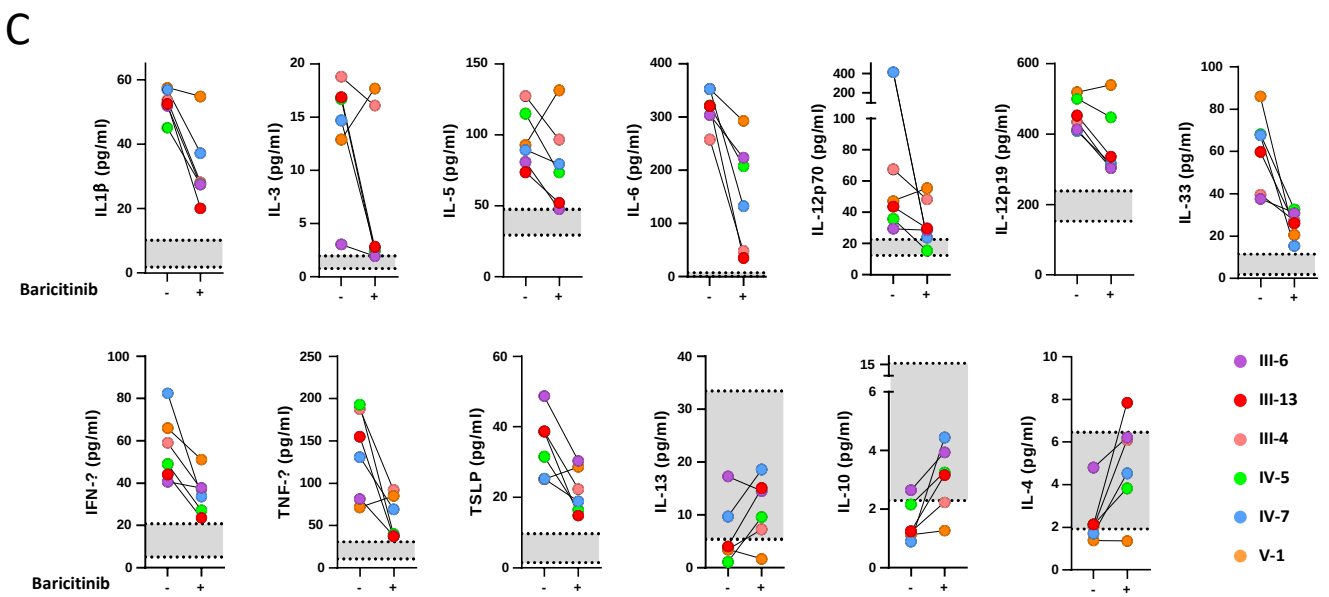
C
IL1β (pg/ml)
IL-3 (pg/ml)
IL-5 (pg/ml)
IL-6 (pg/ml)
IL-12p70 (pg/ml)
IL-12p19 (pg/ml)
IL-33 (pg/ml)
Baricitinib
IFN-? (pg/ml)
TNF-? (pg/ml)
TSLP (pg/ml)
IL-13 (pg/ml)
IL-10 (pg/ml)
IL-4 (pg/ml)
Baricitinib
III-6
III-13
III-4
IV-5
IV-7
V-1

Supplementary Appendix:

Successful treatment of *JAK1* associated inflammatory disease

Antoine Fayand[1,21], Véronique Hentgen[2*], Céline Posseme[3*] ,Carole Lacout[4,21*], Capucine Picard[5], Philippe Moguelet[6], Margaux Cescato[1], Nabiha Sbeih[7], Thomas R.J. Moreau[1], Yixiang YJ Zhu[1], Jean-Luc Charuel[8], Aurélien Corneau[9], Joelle Deibener-Kaminsky[10], Stéphanie Dupuy[11], Mathieu Fusaro[5] ,Benedicte Hoareau[8], Alain Hovnanian[12,13], Vincent Langlois[14], Laurent Le Corre[15], Thiago Trovati Maciel[7], Snaigune Miskinyte[12], Makoto Miyara[8,16], Thomas Moulinet[10], Magali Perret[17], Marie Hélène Schuhmacher[18], Rachel Rignault-Bricard[7], Sébastien Viel[13], Angélique Vinit[9], Angèle Soria[19], Darragh Duffy[3], Jean-Marie Launay[20], Jacques Callebert[20], Jean Philippe Herbeuval[1], Mathieu P Rodero[1§], Sophie Georgin-Lavialle[21§†].

[1] Université Paris Cité, CNRS, Laboratoire de Chimie et de Biochimie Pharmacologiques et Toxicologiques, F-75006 Paris, France.[2] Pediatric Infectious Disease Group (GPIP), Créteil, France; Department General Pediatrics, Centre Hospitalier de Versailles, Le Chesnay, France.[3] Translational Immunology Unit, Institut Pasteur, Université de Paris Cité, Paris, France. [4] Sorbonne University, Genetic Laboratory, Assistance Publique - Hôpitaux de Paris (APHP), Trousseau Hospital, Paris, France. [5] Study Center for Primary Immunodeficiencies, APHP, Necker Hospital for Sick Children, Université de Paris Cité, Paris, France. [6] Department of Pathology, Sorbonne University, Tenon Hospital, APHP, Paris, France. [7] Laboratory of Cellular and Molecular Mechanisms of Hematological Disorders and Therapeutical Implications, Université Paris Cité, Imagine Institute, Inserm U1163, Paris, France. [8] Groupement Hospitalier Pitié-Salpêtrière APHP, Département of immunology, Paris, France. [9] Sorbonne Université, UMS037, PASS, Plateforme de Cytométrie de la Pitié-Salpêtrière CyPS, Paris, France. [10] Department of Internal Medicine and Clinical Immunology, Nancy University Hospital, 5 Rue du Morvan, Vandoeuvre-lès-Nancy 54500, France; UMR 7365, IMoPA, University of Lorraine, CNRS, Nancy, France. [11] BioMedTech Facilities INSERM US36 - CNRS UAR2009 - Université Paris Cité, France. [12] INSERM UMR1163, Laboratory of genetic skin diseases, Imagine Institute, University Paris Cité, Paris, France. [13]Department of Genomics Medicine of Rare Diseases, Hôpital Necker Enfants Malades, AP-HP, Paris, France. [14] Department of Internal Medicine, Jacques Monod Hospital, Le Havre, France. [15] Université de Paris Cité, CNRS, UMR8601, LCBPT, Macromolecular Modeling Platform, Paris, France. [16] Inserm U1135, Centre d'Immunologie et des Maladies Infectieuses (CIMI-Paris), Hôpital Pitié-Salpêtrière, AP-HP, Sorbonne Université, Paris, France. [17] Immunology Laboratory, Lyon Sud Hospital, Hospices Civils de Lyon, University of Claude Bernard-Lyon 1, Lyon, France. [18] Department of Internal Medicine, Emile Durkheim Hospital, Épinal, France. [19] Tenon Hospital, Dermatology-Allergology Department, Sorbonne University, Paris, France. [20] Service of Biochemistry and Molecular Biology, INSERM U942, Hospital Lariboisière, APHP, Paris, France. [21] Sorbonne Université, APHP, Tenon Hospital, department of internal medicine, Paris, France.

***** Contributed equally

§ Codirected the study

[†] Corresponding author: Sophie Georgin-Lavialle : Sorbonne Université, APHP, Tenon hospital, Department of Internal Medicine, National reference center for autoinflammatory diseases and inflammatory amyloidosis (CEREMAIA), Paris, France.

sophie.georgin-lavialle@aphp.fr

CONTENTS

I. Supplementary Methods

Patients and study approval

All adult family members were under care of the same clinician (SGL) and the children of the same paediatrician (VH). As part of their routine care, patients underwent a series of complete physical examinations and underwent several biological, radiological and pathological studies. Cutaneous, articular and digestive disease activities during follow-up were assessed by the treating physician using a subjective scale ranging from 0 (no activity) to 5 (severe involvement). Additionally, all patients, or parents for children, and healthy relatives provided written informed consent for participation, genetic testing and blood samples in accordance with the Declaration of Helsinki and after approval from the ethics committee. An external institutional review board approved the study protocol (CPP Sud Est V, EudraCT number 2018-A01358-47/1).

Collection of blood samples

Blood samples from patients and healthy donors were collected using heparin-coated tubes and with PAXgene Blood RNA tubes (Ozyme). Blood from healthy donors were provided by the "Établissement Français du Sang" (EFS) (convention N°13/CABANEL/089 between "CNRS" and EFS). An informed consent was obtained from all subjects. Serum samples were obtained by centrifugation at 450 x g for 10 min and stored at -80°C. Peripheral blood mononuclear cells (PBMCs) were isolated from fresh whole blood using Ficoll gradient (centrifugation 800 x g for 20 min) and stored in an FCS with 10% DMSO solution at -150°C. PAXgene Blood RNA tubes were stored at -20°C.

DNA extraction and library preparation

DNA was extracted from EDTA-treated peripheral blood samples, either manually by the phenol-chloroform method, or with a Chemagic Prime instrument (Perkin Elmer). Genomic DNA libraries were generated from 2 µg of DNA sheared with a Covaris S2 Ultrasonicator, with the SureSelectXT Library PrepKit [Agilent, Garches, France], on the Genomic Platform at the Imagine Institute, Paris. Capture was performed by hybridization, with 120 bp biotinylated complementary RNA baits designed with SureSelect SureDesign software (Agilent, H. sapiens, hg19, GRCh37, February 2009) that cover approximately 1.095 Mbp encompassing 4136 regions of interest (ROIs) comprising all exons and splicing junctions of the 300 genes selected for study (Table S1). The targeted ROIs were pulled out with magnetic streptavidin beads, amplified by PCR with indexing primers and sequenced on an Illumina HiSeq2500 HT system (paired-end sequencing, 2 x130 bases).

Bioinformatic analysis

Data were analyzed at the Paris University/Imagine Institute's Bioinformatics core facilities. Paired-end sequences were mapped onto the human reference genome (NCBI build37/hg19 version) with the Burrows-Wheeler Aligner. Downstream processing was performed with the Genome Analysis Toolkit (GATK), SAMtools and Picard, according to documented best practices (https://software.broadinstitute.org/gatk/best-practices/). Variant calls were made with the GATK Unified Genotyper, based on the 72nd version of the ENSEMBL database. Genome variants were defined with our in-house PolyDiag software for NGS, which filters out irrelevant and common polymorphisms on the basis of frequencies in public databases: the US National Center for Biotechnology Information Database of Single Nucleotide Polymorphisms (SNPs) (dbSNP), 1000 Genomes, Exome Variant Server (EVS, http://evs.gs.washington.edu/EVS/), and Genome Aggregation Database (GnomAD, https://gnomad.broadinstitute.org/).

NGS and Sanger sequencing

We performed a Next Generation Sequencing (NGS) panel targeting 300 genes causal of PID (23) and 450 genes related to skin diseases. This strategy led to the identification of a heterozygous missense mutation in the exon 19 of *JAK1* gene (NM_002227.4): c.2360 G>T; p.(Cys787Phe). This mutation has never been reported in the GmonAD, dbSNP and HGMD databases. This *JAK1* mutation was confirmed by Sanger sequencing for the index case and several members of his kindred. Primers sequences are available upon request.

Histology

Formalin-fixed, paraffin-embedded tissues were studied. Three-micrometer-thick sections were stained with hematoxylin–eosin–saffron (HES). Immunohistochemical staining was performed, using anti-JAK1 antibody (rabbit polyclonal antibody, each vial containing 100 µg IgG at 1mg/ml, Abcam ab47435) and anti-STAT3 (rabbit monoclonal antibody, each vial containing 100 µg IgG at 1.046 mg/ml Abcam ab76315) at dilution of 1/100 ; anti-CD8, CD31, CD34, CD68, CD99, CD117, AE1/AE3, calretinin, b-catenin, bcl-2, EMA, IgG4, IgG, PS100 (Dako france), STAT6 (Abcam). Deparaffinized sections were stained using a standard avidin–biotin–peroxidase method with diaminobenzidine (DAB) chromogen, and the BOND-III Autostainer (Leica Microsystems, Newcastle-upon, Tyne, UK), after antigen retrieval by heating in the appropriate buffer (pH 6.1 for JAK1 or 9.0 for STAT3, 97°C, for 10 minutes). All skin biopsies were examined and interpreted by the same pathologist (PM).

Cytokine measurements

The biomarker analyses were blinded. Plasma concentrations of IL-1β, IL-3, IL-4, IL-5, IL-6, IL-10, IL-12p70, IL12-p19, IL-13, IL-33, TNF-α, IFN-γ and TSLP were measured using sandwich

immunoassay methods with commercially available electrochemiluminescent detection systems, plates and reagents (V-PLEX human cytokine 30-Plex kits (Meso-Scale Discovery (MSD), Gaithersburg, USA), as per the manufacturer's instructions. Briefly, 50 µL of plasma was loaded per well in the MSD plates. The plates were analyzed using the SECTOR Imager 2400.

Histamine

Blood samples were collected in heparin-coated tubes. After cell lysis by adding 50 µL of blood to 950 µL of distilled water, freezing and thawing twice, and centrifugation at 10,000 × *g* for 10min at 4°C, the supernatant was collected for radioimmunoassay (RIA histamine kit, ref. IM1659, Beckman Coulter). Briefly, histamine in samples, calibrators and controls is chemically modified by acylation. Thereafter acylated histamine is incubated in monoclonal antibody coated tubes in presence of ^{125}I-labeled acylated histamine tracer. Following incubation, the contents of the tubes are aspirated and bound radioactivity is measured in a gamma counter. A calibration curve is established and unknown values are extrapolated from the standard curve.

Cytokine stimulation and treatment of PBMC/whole blood

PBMCs or whole blood cells were incubated at 37°C with IFN-α2 (100 UI/mL), IL-2 (50 ng/mL), IL-4 (50 ng/mL), IL-6 (10 ng/mL) or IFN-γ (400 UI/mL) for 30 min. Cellular response was then assessed using fluorescence activated cell sorting (FACS) or mass cytometry (CyTOF) (see below). For treated conditions, cells were incubated at 37°C with baricitinib (200 nM) for 15 min prior to cytokine stimulation.

Flow cytometry

For the study of STATs phosphorylation

The phosphorylation of STAT1, STAT3, STAT5B and STAT6 were assessed in PBMCs (1 million cells per condition) from patients and healthy donors at basal state and after cytokine stimulation with or without baricitinib. We used the PerFix EXPOSE kit (Phospho-Epitopes Exposure kit, Beckman Coulter) according to the manufacturer's instructions except for the staining of membrane antigens, which was carried out before cell fixation. Membrane antigen staining was achieved using two different mixes of fluorochrome-conjugated antibodies (Table S4). Mix 1 was used for experiments with IFN-α2 and IL-2 stimulations, whereas mix 2 was used for experiments with IL-4 and IL-6 stimulations.

Cells were then fixed and permeabilized. Finally, staining of intracellular STATs was performed using anti-pSTAT1-AF488 (clone 4a, BD Biosiences), anti-pSTAT3-VB500 (clone REA324, Miltenyi Biotec), anti-pSTAT5b-PE (clone SRBCZX, Life technologies) and anti-pSTAT6-PE (clone REA413, Miltenyi Biotec). After washing, samples were acquired on a Attune NxT cytometer (ThermoFisher). FACS data were analysed with Kaluza software (Beckman Coulter). The following gates were applied before the identification of specific cell types: FSC-A / SSC-A and FSC-H / FSC-A for exclusion of doublets. We defined the following specific cell types: classical monocytes (CD14+ CD16-), inflammatory monocytes (CD14dim CD16+), naive B-cells (CD19+ IgD+), memory B-cells (CD19+ IgD-), CD4 T-cells (CD3+ CD8- with mix 1; CD3+ CD4+ with mix 2), CD8 T-cells (CD3+ CD8+), immature NK-cells (CD56bright CD16-) and mature NK-cells (CD56dim CD16+). Mean fluorescent intensity (MFI) of each pSTAT specific antibody-fluorochrome was then assessed in each cell type. The effect of cytokine stimulation with or without baricitinib on phosphorylation of STATs is given as fold-increase of MFI pSTATx after stimulation over unstimulated level.

For measure of activation markers on basophils

Peripheral blood basophils from patients and controls were stained and analyzed by conventional flow cytometry in a Gallios (Beckman-Coulter) cytometer using FlowJo software. The following labeled human antibodies were used: eF506 anti-CD45 (clone HI30, eBioscience), eF450 anti-FcεRIα (clone AER-37, eBioscience), PE anti-CD123 (clone 6H6, eBioscience), APC-Cy7 anti-CCR3 (clone 5E8, BioLegend®), APC anti-CD203c (clone NP4D6, eBioscience), PE-Dazzle594 CD107a (clone H4A3, BioLegend®), PE-Cy7 CD69 (clone FN50, BioLegend®), PerCP-Cy5.5 CKit (clone A3C6E2, BioLegend®), and FITC anti-CD63 (clone H5C6, BioLegend®). Basophils were defined as FcεRI CD123 CCR3 positive cells and CKit negative cells.

Mass cytometry

In addition to phosphoflow, CyTOF was performed to assess the phosphorylations of STAT1, STAT3, STAT4, STAT5b and STAT6 as well as NFκB in whole blood (300 µL per condition) of patients and healthy donors at basal state and after cytokines stimulation. First experiments were performed using the PerFix EXPOSE kit (Phospho-Epitopes Exposure kit, Beckman Coulter) with the same amendment to the manufacturer's protocol: 1- labelling of membrane antigen with metal-isotope-tagged antibodies (Table S5), 2- fixation, 3- permeabilization and 4- labelling of intracellular antigens (Table S5). In a second set of experiments the phosphorylations of STAT1, STAT3, STAT5b and STAT6 were evaluated as follow: 1-labelling of membrane antigen with metal-isotope-tagged antibodies (Table S4, but

instead of CD38-144Nd, CD38-172Yb 5HIT2 clone was used – Fluidigm), 2-fixation using Protein Stabilizer Prot1 (SmartTube Inc.), 3-permeabilisation using a thaw-lyse buffer (SmartTube Inc.) and pure methanol, 4-labelling of intracellular antigens (Table S4). For both experiments, after washing of tagged antibodies targeting intracellular antigens, samples were resuspended in PBS with 2% formaldehyde (Thermo scientific) and 125 nM of Cell-ID™ Intercalator-Ir (Fluidigm) and incubated at 4°C overnight. Samples were then stored at -80°C. Cells were washed twice in PBS+0.5% SVF and then washed and resuspended in Maxpar cell acquisition solution, a high ionic strength solution, at a concentration of 1 million cells per ml and mixed with 10% EQ beads (for sample standardisation) just prior to acquisition.

Cell events were acquired on the Helios mass cytometer (DVS sciences) and CyTOF software version 6.7.1014 (Fluidigm, Inc Canada) at the "Plateforme de Cytométrie de la Pitié-Salpêtrière (CyPS)". An average of 250,000 events were acquired per sample. The standard mass cytometry files (fcs3.0) produced by HELIOS were normalised using the CyTOF software. This method normalises the data to a global standard determined for each log of EQ beads. CyTOF data were analysed with OMIQ (Omiq, Inc.). The analysis was conducted on CD25+ and CD25low viable cells only. Each of the three patients and the three healthy donors were analysed individually, as well as the 3 healthy donors concatenated. Blood leukocyte populations and sub-populations were identified using unsupervised clusterisation with the FlowSOM algorithm. A first FlowSOM run (xdim=12, ydim=12, rien=10, distance metric=euclidean, random seed=6025) allowed us to identify clusters corresponding to granulocytes, which were subsequently excluded from subsequent analysis. A second FlowSOM run (xdim=10, ydim=10, rien=10, distance metric=euclidean, random seed=506) was used to generate a new set of clusters organised in a spanning tree. According to their phenotypes, clusters were manually distributed in metaclusters corresponding to leukocyte populations and sub-populations. As a quality control we performed dimensionality reduction using flt-SNE (perplexity: 60; Theta: 0.8, Random Seed: 3173; Max iteration: 2000; all other: default settings) to manually gate on CD56+ NK cells. For each patient, donor or group of donors, the effect of cytokine stimulations in each cluster or gate, expressed as fold-increase of phosphoprotein signal, was displayed on the spanning tree or as histogram plots.

Multiplexed gene expression analysis

Starting from PAXgene Blood RNA tubes (Ozyme), RNA of healthy donors and patients (before and after treatment with baricitinib) was extracted using Quick-RNA Whole Blood kit (Zymo Research). Samples were stored at -20°C. After thawing, quantity of RNA was measured with the Qubit RNA High Sensitivity kit (Life Technologies). A total of 100 ng RNA per sample was used to assess the expression of 750 genes involved in immunity with the nCounter Human Autoimmune Profiling Panel (Nanostring). Expression data were normalized using the nSolver software (Nanostring) in 3 steps: 1-

subtraction of geometric mean of negative probes, 2- normalization of data using geometric mean of positive probes and 3- normalization of data using housekeeping genes selected with the geNorm algorithm. Differential gene expression analysis was conducted in R (R Core Team, 2020) with "broom" package, using multiple linear regression. Gene set enrichment analysis was conducted in GSEA (version 4.1.0, Broad Institute) using pathway annotations from Biocarta database and the following parameters: number of permutations= 2000, enrichment statistic = classic, min set size = 5, max set size = 200 and all others set to default. Figures were produced using Prism software, version 9.1.1 (version 9.1.1, GraphPad).

ISG score:

200ng of RNA were hybridized to the probes (a reporter probe and a capture probe) at 67°C for 16–21h using a thermocycler. Samples were then inserted into the nCounter Prep Station for the removal of excessive probes, purification and immobilization onto the internal surface of a sample cartridge for 2–3h. Finally, the sample cartridge was transferred to the nCounter Digital Analyzer where color codes were counted and tabulated for each target molecule. Count number obtained for the 6 ISGs were normalized by the geometric mean of 3 housekeeping genes count number (β-Actin, HPRT1 and POLR2A) as well as the negative and positive controls values using nSolver software. The relative expression was determined for each normalized ISG expression dividing by the median normalized expression of each ISG from a control group. Finally, the median relative expression of these 6 ISGs was used to calculate the IFN score.

RNA sequencing

Fastq files were then aligned using STAR algorithm (version 2.7.6a), on the Ensembl Homo sapiens GRCh38 reference, release 101.

Reads were then count using RSEM (v1.3.1) and the statistical analyses on the read counts were performed with R (version 3.6.3) and the DESeq2 package (DESeq2_1.26.0) to determine the proportion of differentially expressed genes between two conditions.

We used the standard DESeq2 normalization method (DESeq2's median of ratios with the DESeq function), with a pre-filter of reads and genes (reads uniquely mapped on the genome, or up to 10 different loci with a count adjustement, and genes with at least 10 reads in at least 3 different samples). Following the package recommendations, we used the Wald test with the contrast function and the Benjamini-Hochberg FDR control procedure to identify the differentially expressed genes.

R scripts and parameters are availables on GitHub (https://github.com/BSGenomique/genomic-rnaseq-pipeline/releases/tag/v1.0420

Cell sorting

Peripheral blood mononuclear cells (PBMCs) and polynuclear cells (PN) were isolated from blood using Percoll (GE Healthcare) density gradient. Briefly, 100% isotonic Percoll was made by 1/10 dilution of 10X PBS in Percoll. 85%, 80%, 75%, 70% and 65% isotonic Percoll solutions were made by dilution in PBS and 2ml of each solution were layered from the higher to the lower density in Falcon-15 tubes. Whole blood from patients or healthy donors was spun for 10 minutes at 450 x g. Buffy coat was collected at the interface between red blood cells and plasma. 5ml of buffy coat was layered on top of the Percoll gradient. Tubes were centrifuged for 20 minutes at 800 x g with no brake.

The cell layer at the interface between the 65% Percoll solution and PBS (PBMC enriched faction) and cells at the interface between the 65% and 70%, the 70% and 75%, and the 75% and 80% fraction (PN enriched fraction) were collected and washed in PBS. Remaining red blood cells from the PN enriched fraction were lysed by 10 second incubation in 9ml of water followed by addition of 1ml of 10X PBS.

PBMCs enriched cells were labelled with CD3 APC (Miltenyi, REA613), CD19 PE-Cy7 (Invitrogen, SJ25C1), CD56 PE (Biolegend, 5.1H11) and CD14 APC AF750 (Beckman Coulter, RMO52). PN enriched cells were labelled with CD16 APC (Miltenyi, REA423), CD123 FITC (Miltenyi, REA918) and HLADR PcP-Cy5 (Biolegend, L243). PBMC and PN subsets were isolated using a BD FACS Aria II according to the gating strategy defined in Fig. S17. After sorting, cells were pelleted, and stored at −80 °C until analysed for histamine content.

Protein modelling: PDB reference

The Impact of the C787F mutation on protein stability was evaluated using the calculated mutation energy protocol implemented in Discovery Studio (DS) 2016 (24). The negative value of the mutation energy (-0.75 kcal.mol^{-1}) calculated for C787F mutant corresponds to a stabilizing effect. Furthermore, a model structure of mutated C787F human JAK1 was built using the Built Mutants protocol incorporated in DS 2016 (25). In this model, the mutated C787F residue formed new interactions with C817 and Y788.

Autoimmunity Panel

Indirect Immunofluorescence on HEp-2000™ cells and rat tissues.

Serum samples from all participants were subjected to the ANA-test and anti-rat kidney, stomach and liver tissue test using commercial slides (Immunoconcept) and a PhD system

immunoassay (Biorad). HEp-2000™ are HEp-2 cells with overexpressed Ro60 antigens. Serum samples were diluted in PBS buffer and incubated for 25 minutes at room temperature in a moist chamber. After washing twice in PBS, cells were incubated with fluorescein isothiocyanate conjugated goat anti–human IgG, Ig heavy and light chains, Immunoconcept for ANA-test and anti-human polyvalent immunoglobulins, Biorad for anti-rat tissue for another 25 minutes in the dark. After washing twice as before, slides were counter-stained with Evans blue and assembled with glycerol and coverslips.

Statistics

All statistical analyses were performed using GraphPad Prism (version 9.1.1). As indicated in the Figures, results were analyzed in a two-tailed, unpaired or paired Student's *t* test, or a two-sided Mann–Whitney U test. For all analyses, the threshold for statistical significance was set to $p < 0.05$.

Sup Figure 1

Figure S1

Clinical aspects of several family members. A: Face involvement of atopic dermatitis in, from left to right, patients V-4, IV-9, IV-5 and II-16. B: Details of the eyelid dermatitis with Dennie-Morgan fold in, from left to right, patients V-4, IV-9, IV-5, and II-16. C: Hands of patients IV-9 (left) and III-13 (right) with ichthyosis, , lichenification and wart sequela. D: Ichthyosis and lichenification involvement of feet from several patients (left to right: V-1, IV-9, III-4, II-16). E: From left to right: atopic dermatitis of the wrist of patient V-1, atopic dermatitis inside the bend of the elbow of patient V-5, and inflammatory linear verrucous epidermal papules of the forearms of patients IV-5 and III-4.

Sup Fig 2

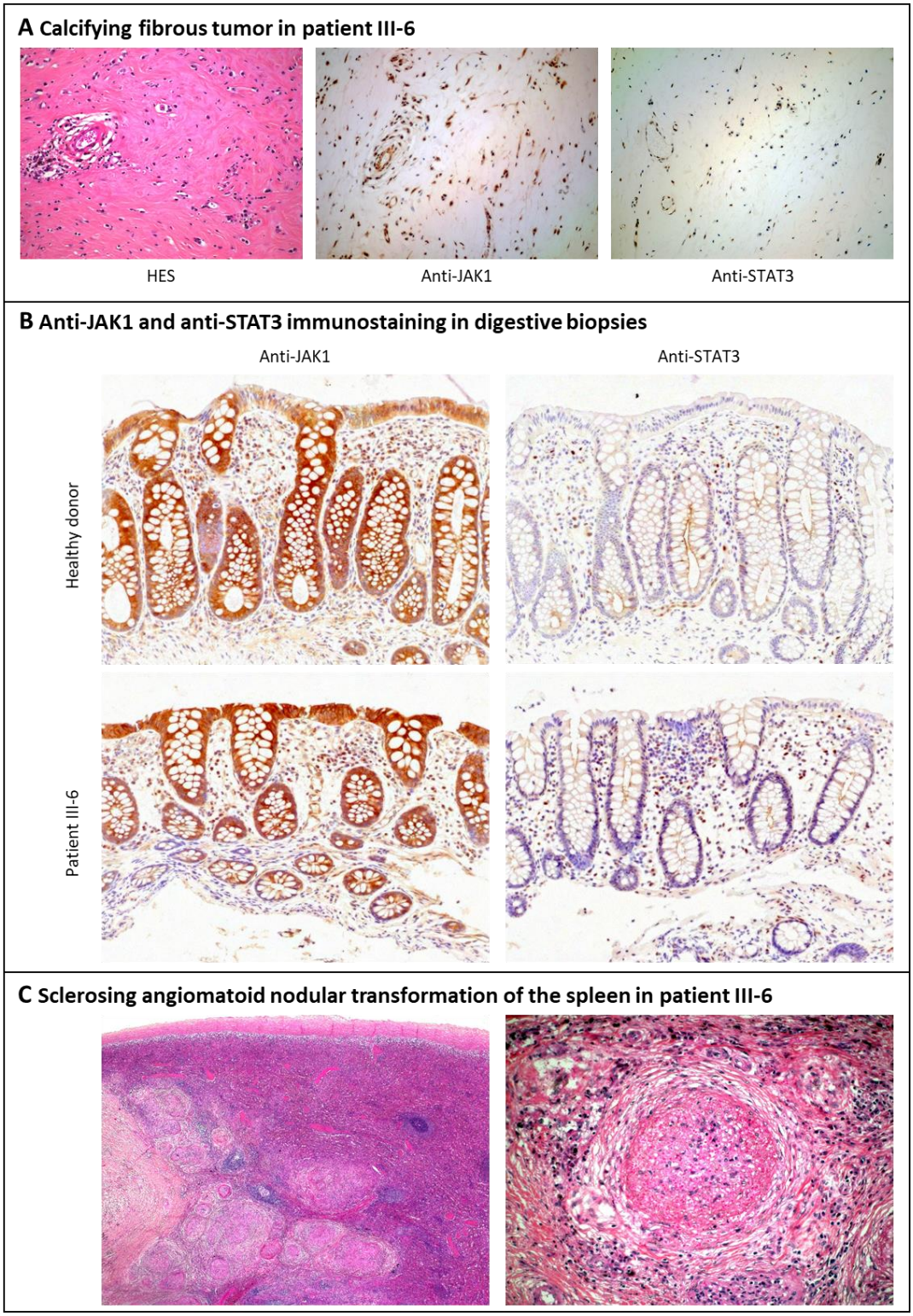

Figure S2 Pathological findings

A) Pathological characteristics of calcifying fibrous tumours including, from left to right, HES x200: fibrosis with fibroblastic proliferation and inflammatory infiltrate; JAK1 staining x200: high cytoplasmic JAK1 expression in endothelial and fibroblast cells; STAT3 staining x200: high nuclear STAT3 expression in endothelial and fibroblast cells. **B**) Anti-JAK1 and anti-STAT3 immunostaining of digestive biopsies from healthy donors and patient III-6, showing no difference. **C)** Pathological characteristics of the sclerosing angiomatoid nodular transformation of the spleen (SANT) in patient III-6 with, from left to right, HES x20: multinodular mass in the red pulp and HES x200: single angiomatoid nodule with central vascular spaces lined by plump endothelial cells, surrounded by a ring of fibrosis.

Sup Fig 3

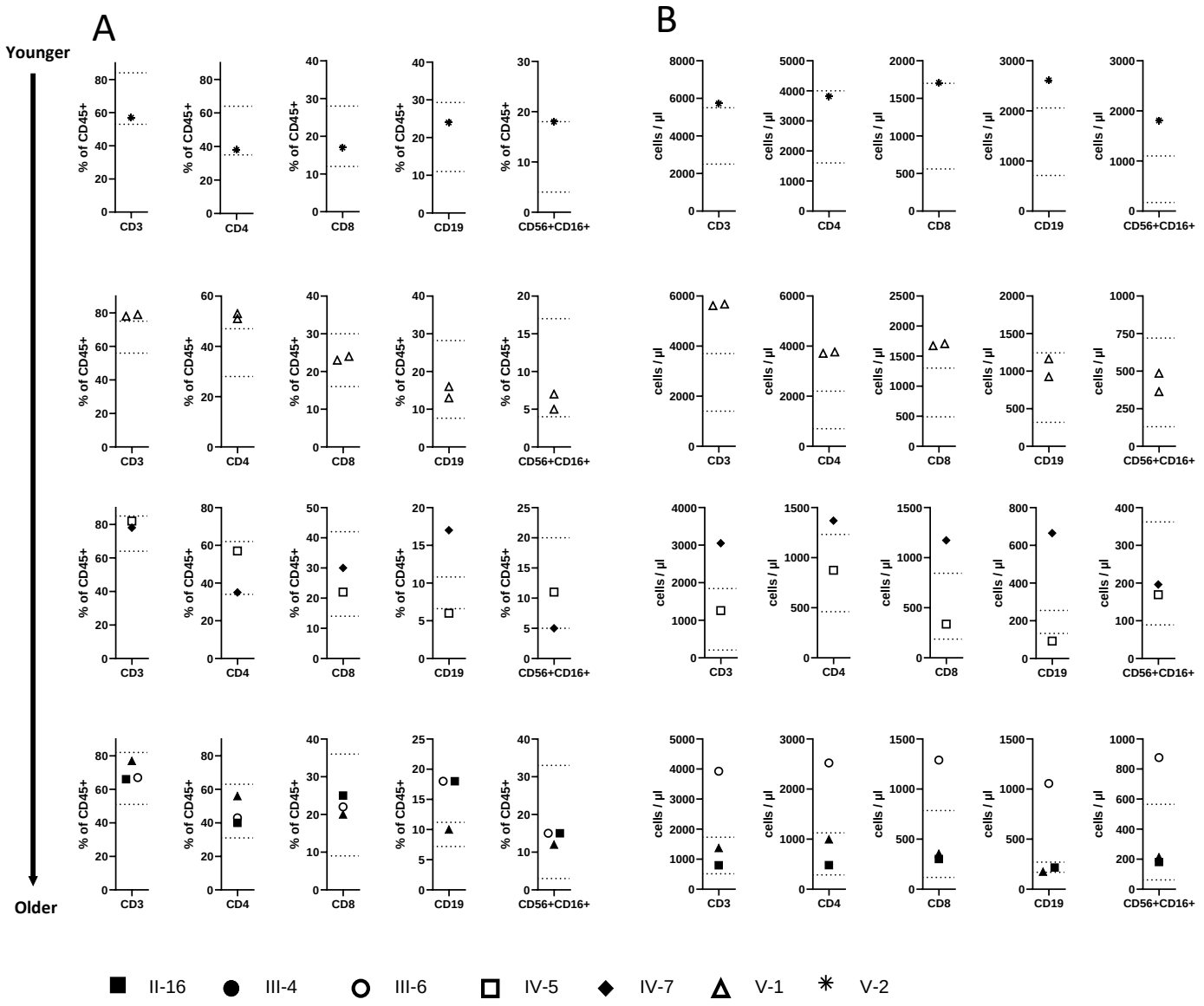

Figure S3: Clinical immunophenotyping of patients. Representation of **A)** the proportion and **B)** the number of the main leukocyte population in patients. Dot lines represent distribution ranges in age-paired healthy individuals.

Sup Fig 4

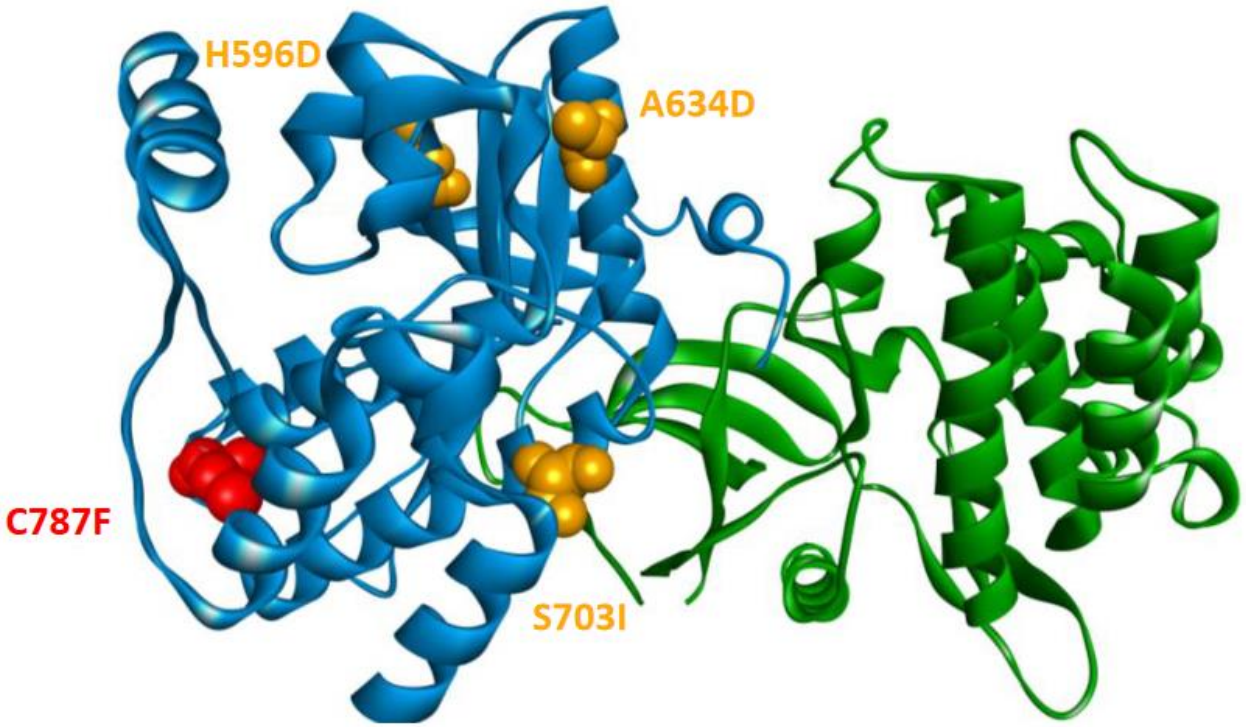

Figure S4 : Modeling of kinase and pseudokinase domains of JAK1.
3D modelling of JAK1 pseudo Kinase domaine **(Blue)** and Kinase domain **(Green)** with previously describe mutation in orange, and the novel mutation in red.

Sup Fig 5

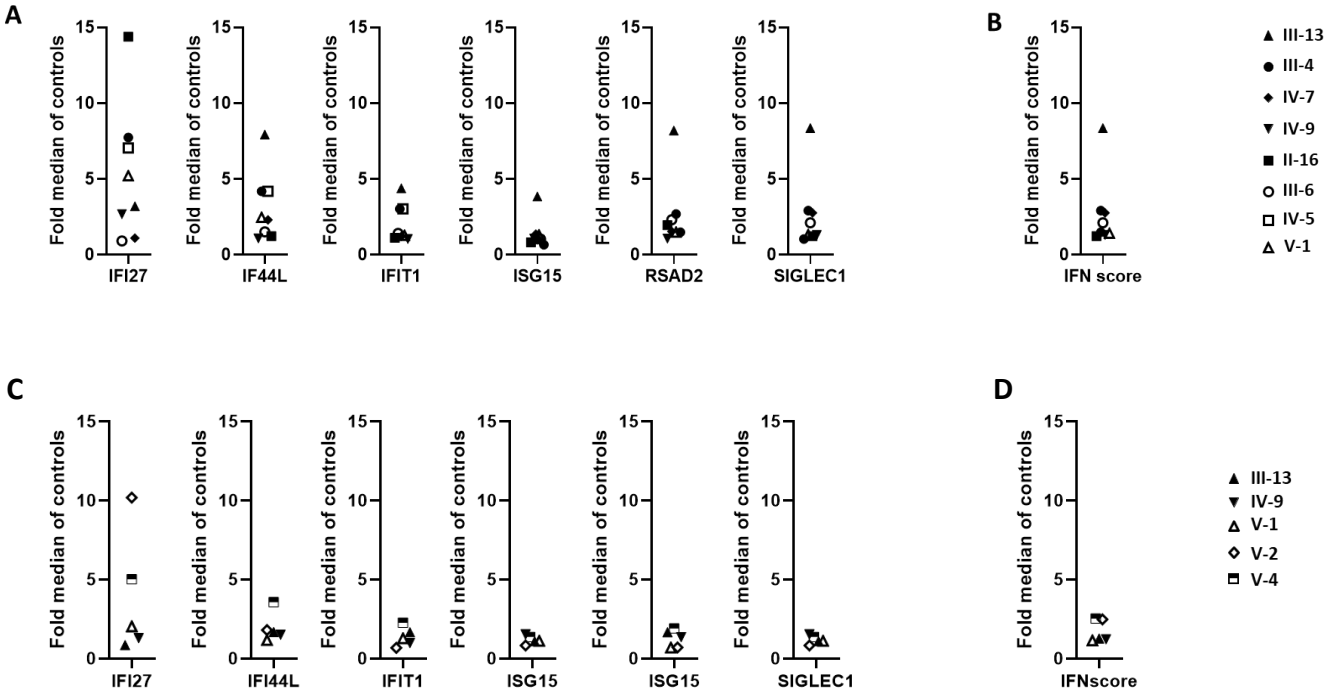

Figure S5: Type 1 interferon signature

A) Quantification by Nanostring of 6 ISGs from blood of JAK1 patients, B) Type I interferon score calculated as the median fold increase of the 6 tested ISGs from Nanostring experiments. C) Quantification by RNAseq of 6 ISGs from blood of JAK1 patients. D) Type I interferon score calculated as the median fold increase of the 6 tested ISGs from RNAseq experiments. IV-7 was treated with baricitinib at the time of sampling.

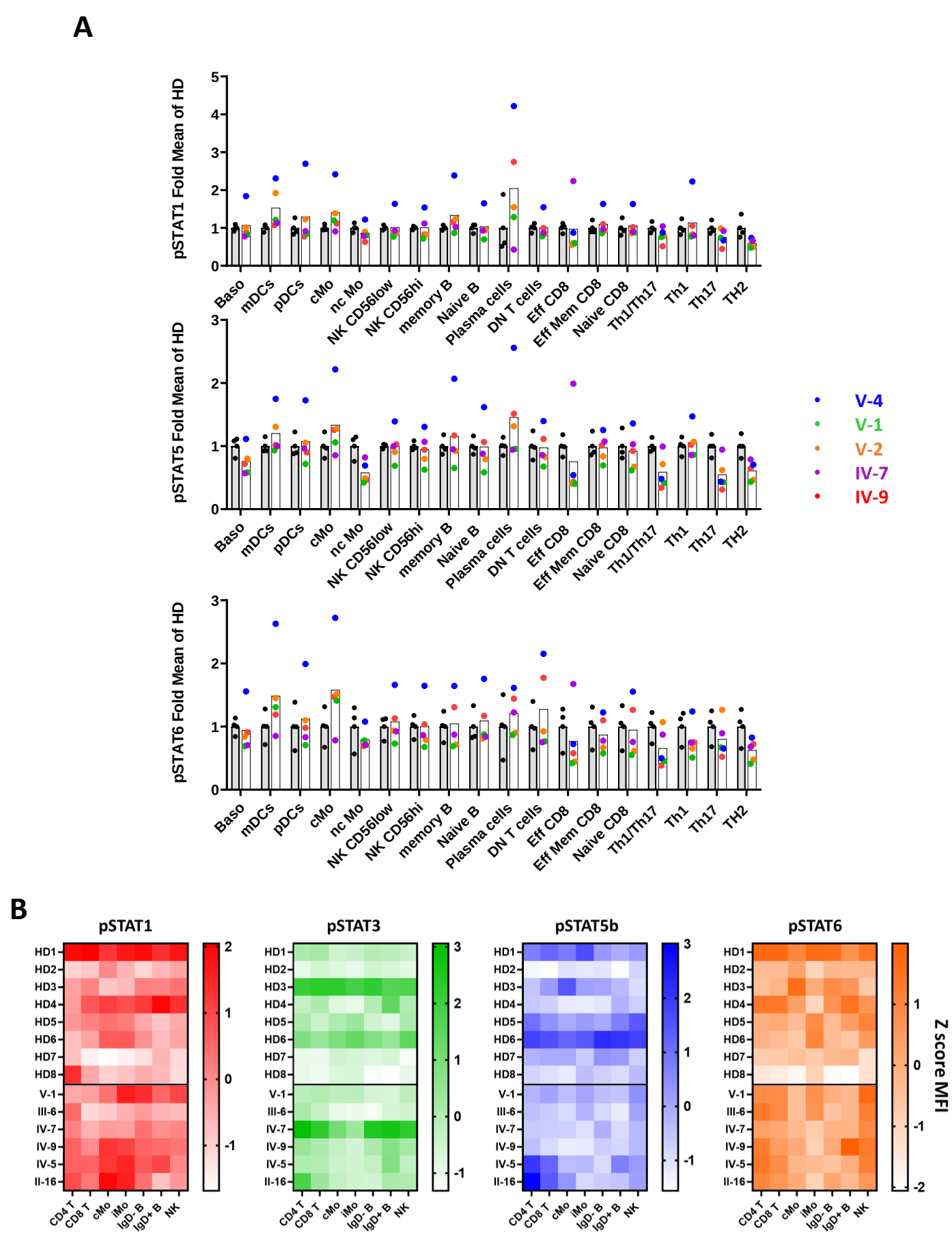

Figure S6: Basal pSTAT1, pSTAT3, pSTAT5b and pSTAT6 levels in leukocytes JAK1 patients. Bar graph representations of the phosphorylation status of STAT1, STAT5b and STAT6 on unstimulated fresh whole blood from 4 donors and 5 untreated patients. For IV-7 : Baricitinib discontinuation >72h.B: Heat mat representation of the phosphorylation status of STAT1, STAT3, STAT5b and STAT6 in unstimulated frozen PBMCs from 8 healthy donors and 6 patients measured by flow cytometry.

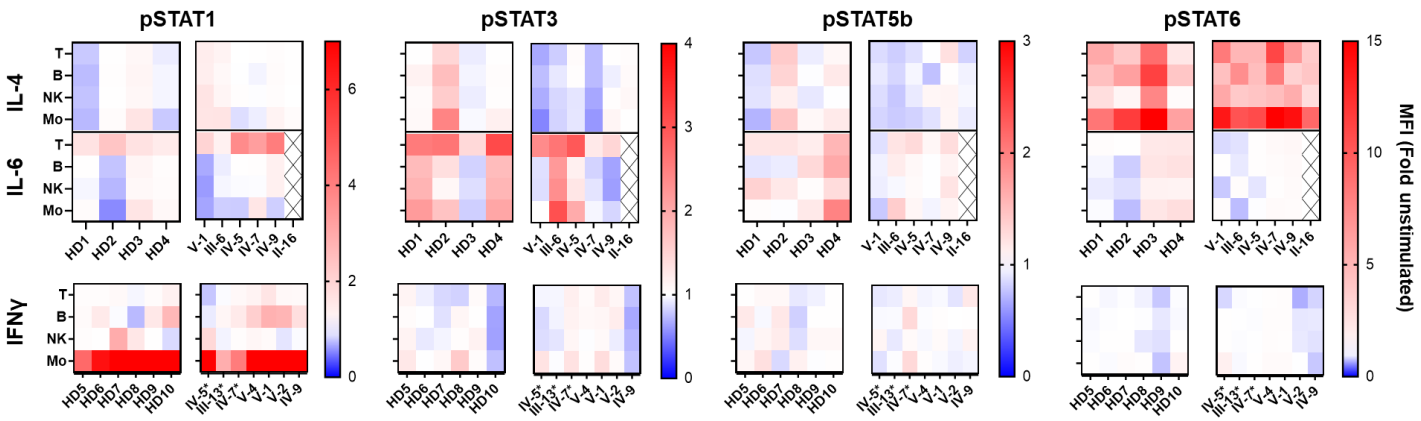

Figure S7 : Phosphorylation status of STAT1, STAT3, STAT5b and STAT6 was measured by flow cytometry on frozen PBMCs from 6 healthy donors and 7 patients stimulated with IFN-γ (400 UI/mL), IL-4 (50 ng/mL) or IL-6 (10 ng/mL) for 30 min. *sample from patients treated with JAK inhibitors..

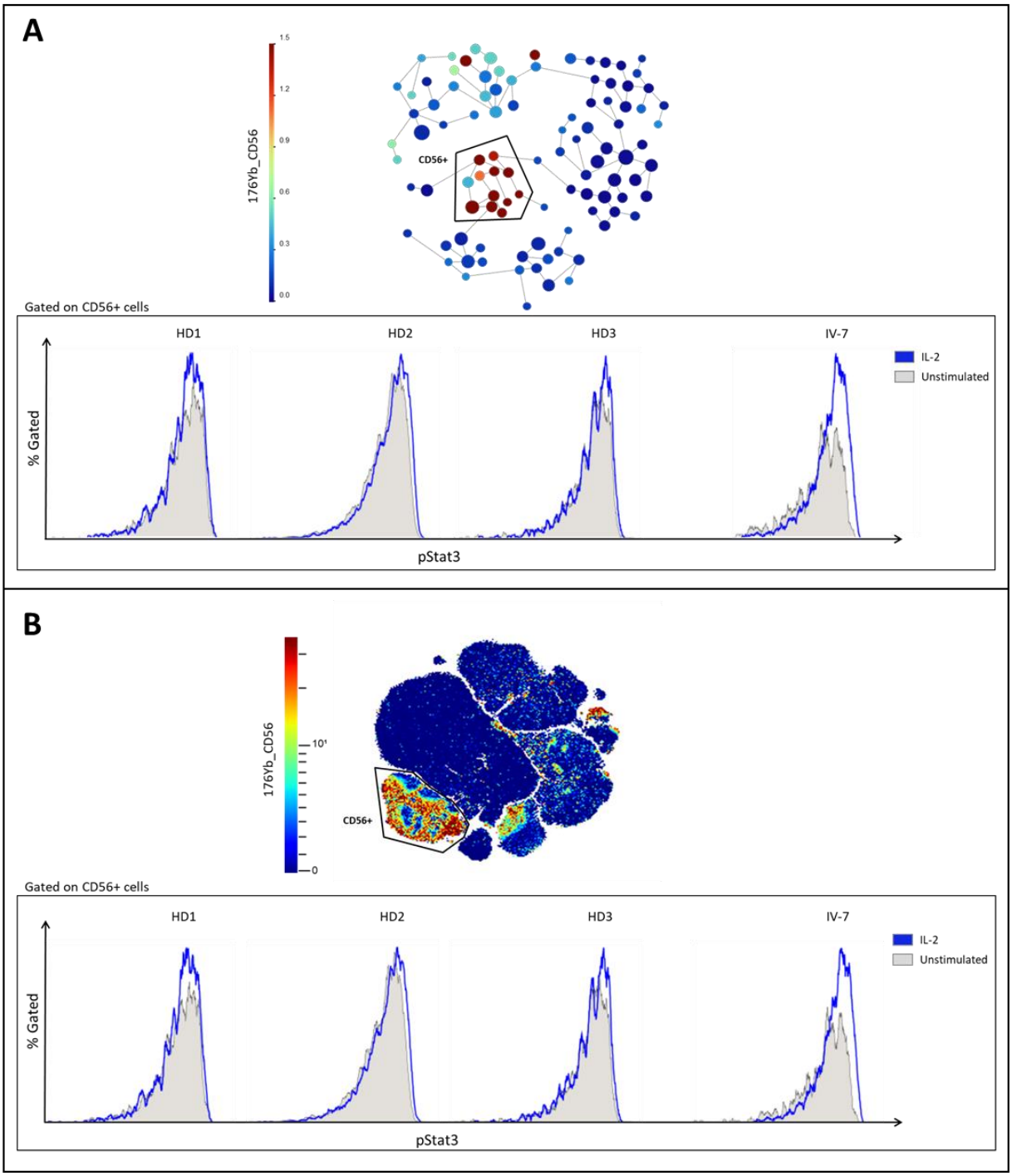

Figure S8: STAT3 phosphorylation in NK cells from patient IV-7 and healthy donors whole blood in response to stimulation with interleukin 2: Phosphorylation status of STAT3 was measured by mass cytometry on whole blood from 3 healthy donors and patient IV-7 stimulated with IL-2 (50 ng/mL). CD56+ NK-cells were gated using two algorithms: FlowSOM (panel A) and tSNE (panel B). On both the spanning tree (FlowSOM, panel A) and the scatterplot (tSNE, panel B), the colored continuous scale indicates the intensity of the CD56 marker. Histograms depict the pSTAT3 intensity in NK-cells identified using FlowSOM (panel A) and tSNE (panel B) either at basal state (grey) or following IL-2 stimulation (blue). Stimulation with IL-2 induced no phosphorylation of STAT3 in NK-cells from healthy donors whereas an increase was observed in those from the patient.

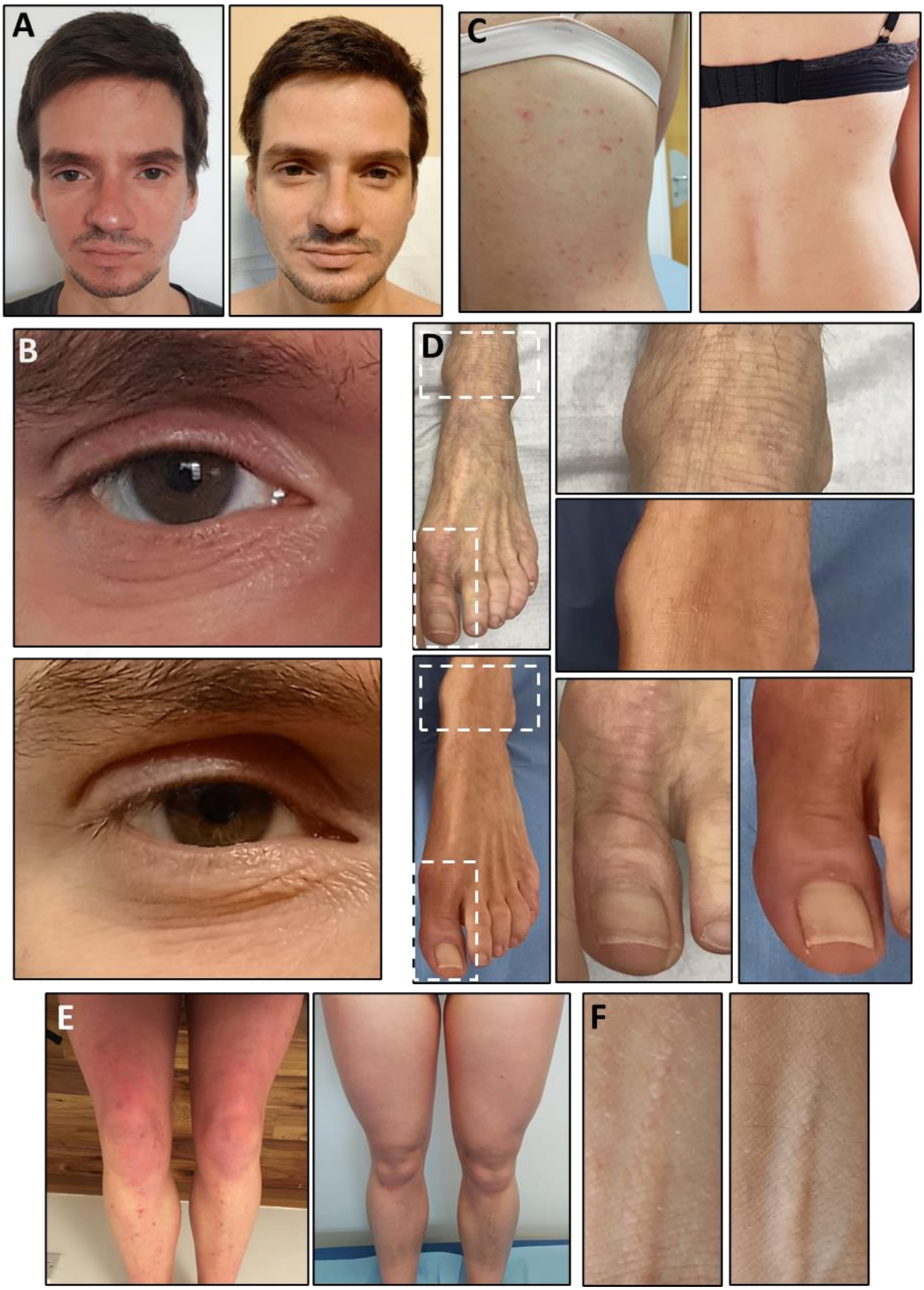

Figure S9: Clinical response to JAK inhibitors

Evolution of various skin manifestations of the disease under treatment with a JAK inhibitor: **A:** Improvement of facial inflammatory lesion-under treatment (right) compared to before treatment (left) in patients IV-5 (top). **B:** Improvement of eyelid dermatitis of patient IV-5 (untreated = left, treated = right).**C :** Resolution of neutrophilic prurigo-like exanthema of the trunk of patient IV-7 (untreated = left, treated = right) **D:** Good response of lichenification illustrated by a focus on patient III-13's left foot (untreated = top, treated = bottom) with focus on the first toe and the ankle. **E:** Resolution of neutrophilic infiltrated exanthema of the legs of patient IV-7 (untreated = left, treated = right) **F:** Improvement of inflammatory linear verrucous epidermal papules of the forearm of patient IV-5 (untreated = left, treated = right).

Sup Fig 10

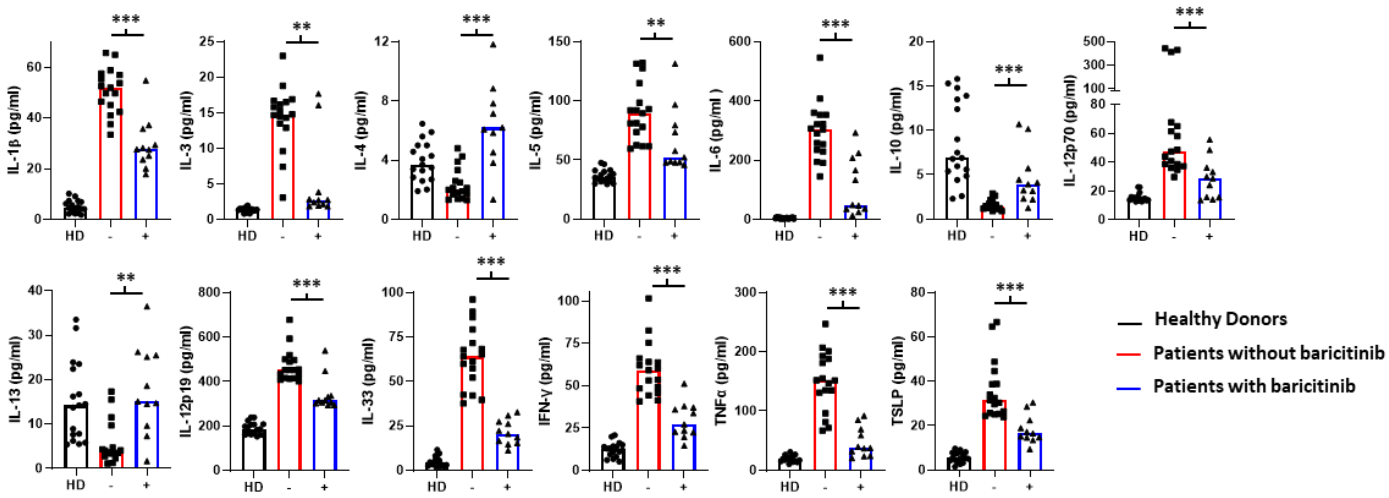

Figure S10: Correction of Cytokine circulating levels by baricitinib in patients. Representation of all the cytokine measurements performed in JAK1 patients before initiation of a treatment by JAK inhibitor or during treatment with baricitinib.

Sup Fig 11

A Gene set enrichment analysis comparing patients treated with baricitinib and healthy donors

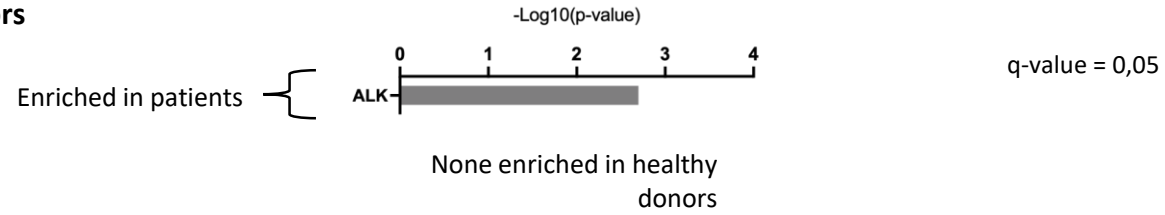

B ALK pathway gene expression

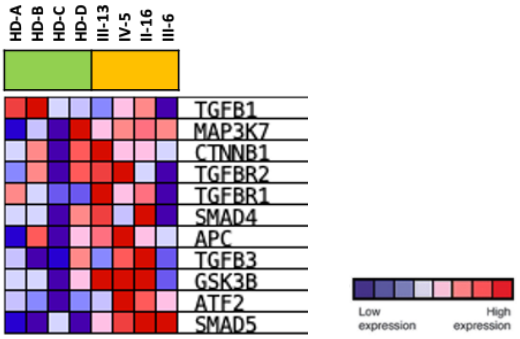

Figure S11: Transcriptomic signature of patients after initiation of JAK inhibitor treatments

A) Significantly enriched pathways in whole blood from patients after initiation of baricitinib (> 7 months) compared to healthy donors **B)** Detail of the genes from the identified pathway.

Sup Fig 12

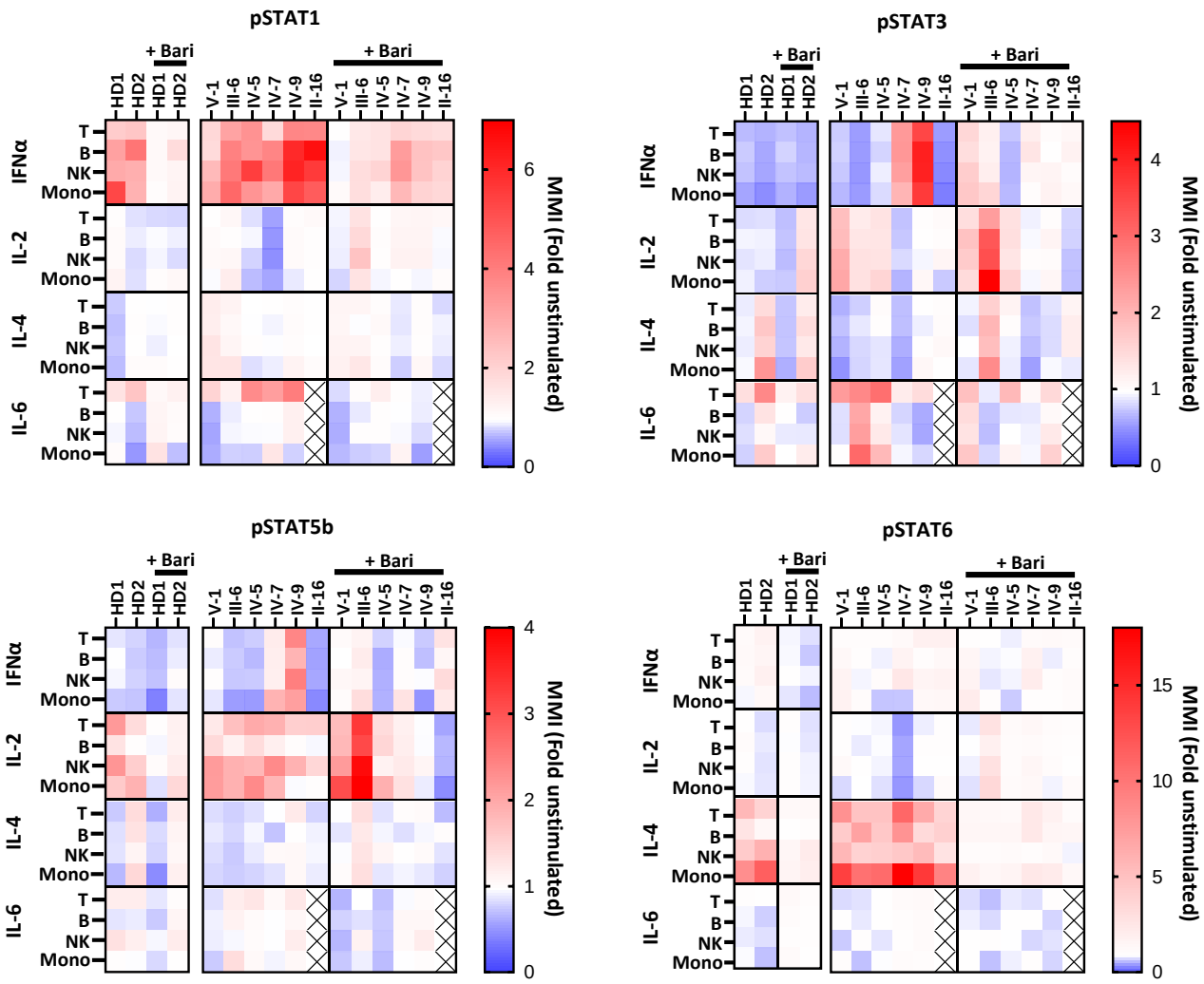

Figure S12: STAT1, STAT3, STAT5b and STAT6 phosphorylation in patients and healthy donors PBMCs following various cytokine stimulations and in vitro treatment with baricitinib.

Phosphorylation status of STAT1, STAT3, STAT5b and STAT6 were measured by flow cytometry on frozen PBMCs from 4 healthy donors and 6 patients stimulated with IFN-α2 (100 UI/mL), IL-2 (50 ng/mL), IL-4 (50 ng/mL) or IL-6 (10 ng/mL) for 30 min.

Sup Fig 13

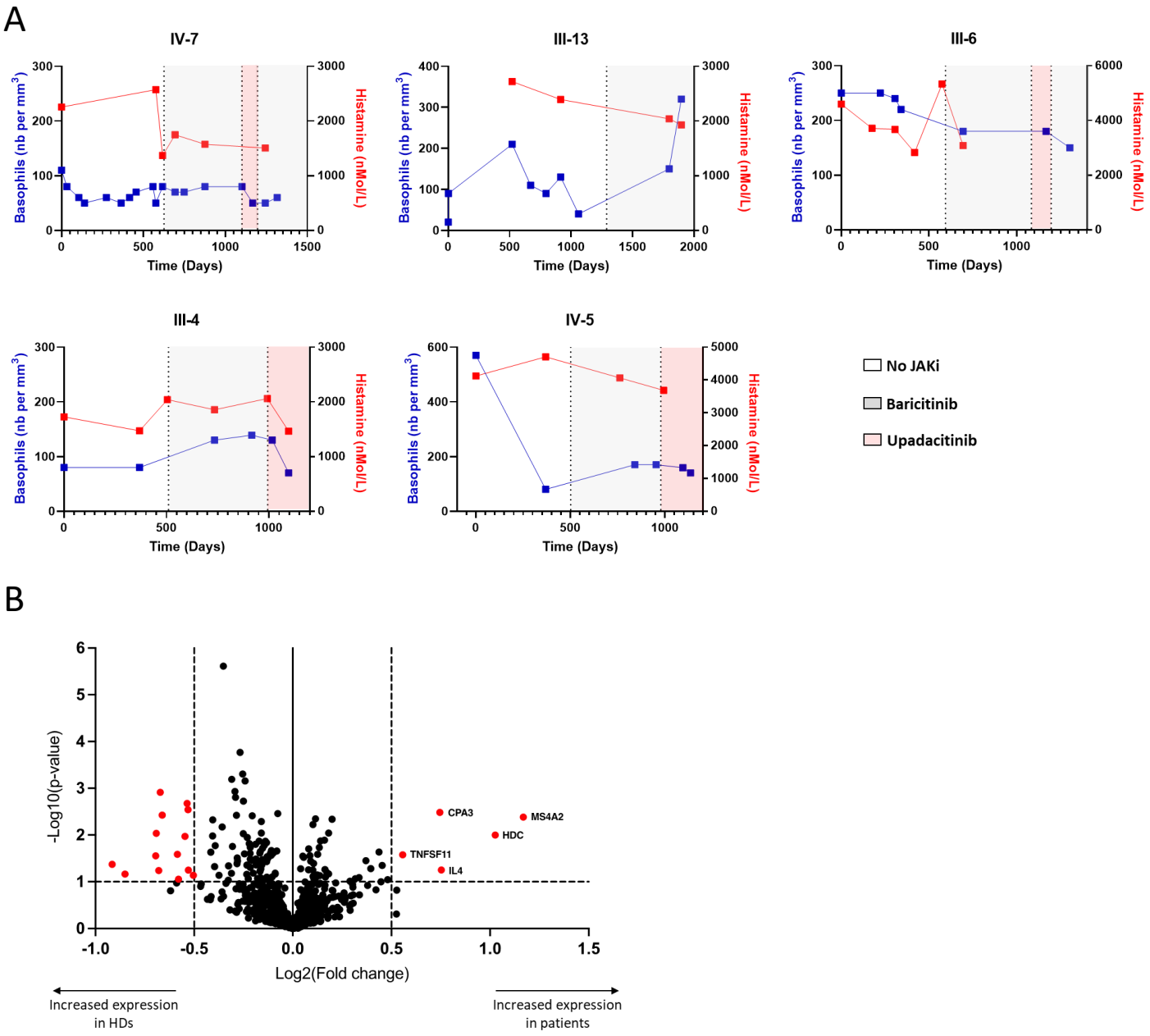

Figure S13: Sustained basophilia under JAK inhibitor treatments. A) Follow up of blood basophil counts and blood histamine levels in patients treated with baricitinib (grey) or upadacitinib (light red). **B)** Volcano plot representation of the gene expression analysis comparing treated patients (> 7 month) to healthy donors. Basophil related genes are among the top upregulated genes in treated patients.

Sup Fig 14

Figure S14: Control of canonical STAT phosphorylation by JAK inhibitors. Spanning tree representation of the phosphorylation status of STAT1 after IFNα stimulation and STAT5b after IL-2 stimulation on unstimulated fresh whole blood from 3 donors and V-1 after initiation of baricitinib treatment (11 months) and IV-5 after initiation of upadacitinib treatment (2 months).

Figure S15

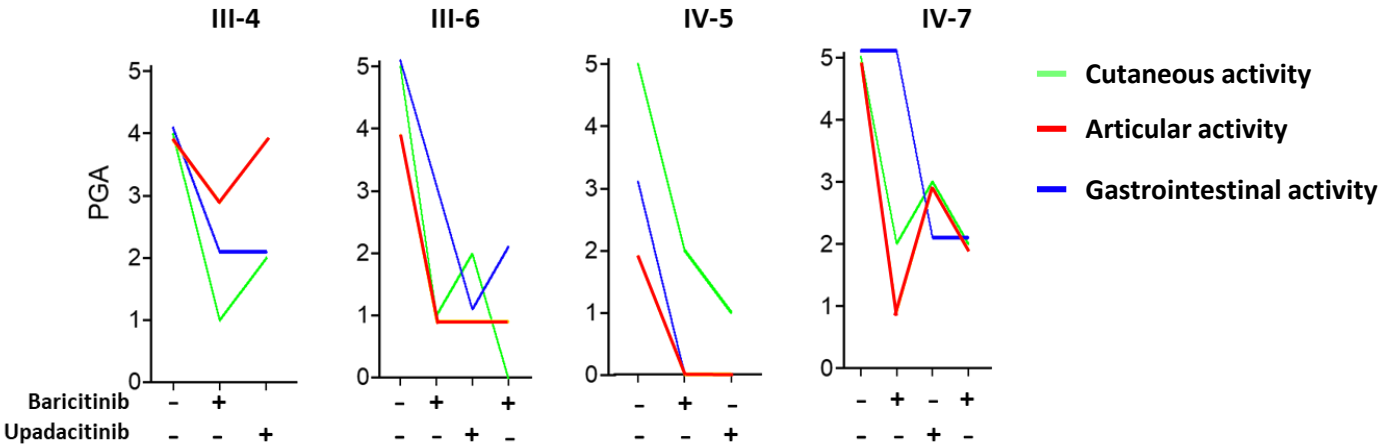

Figure S15: Response to upadacitinib.
Physician assessment score for the three main clinical features following treatment with baricitinib and upadacitinib**.**

Sup Fig 16

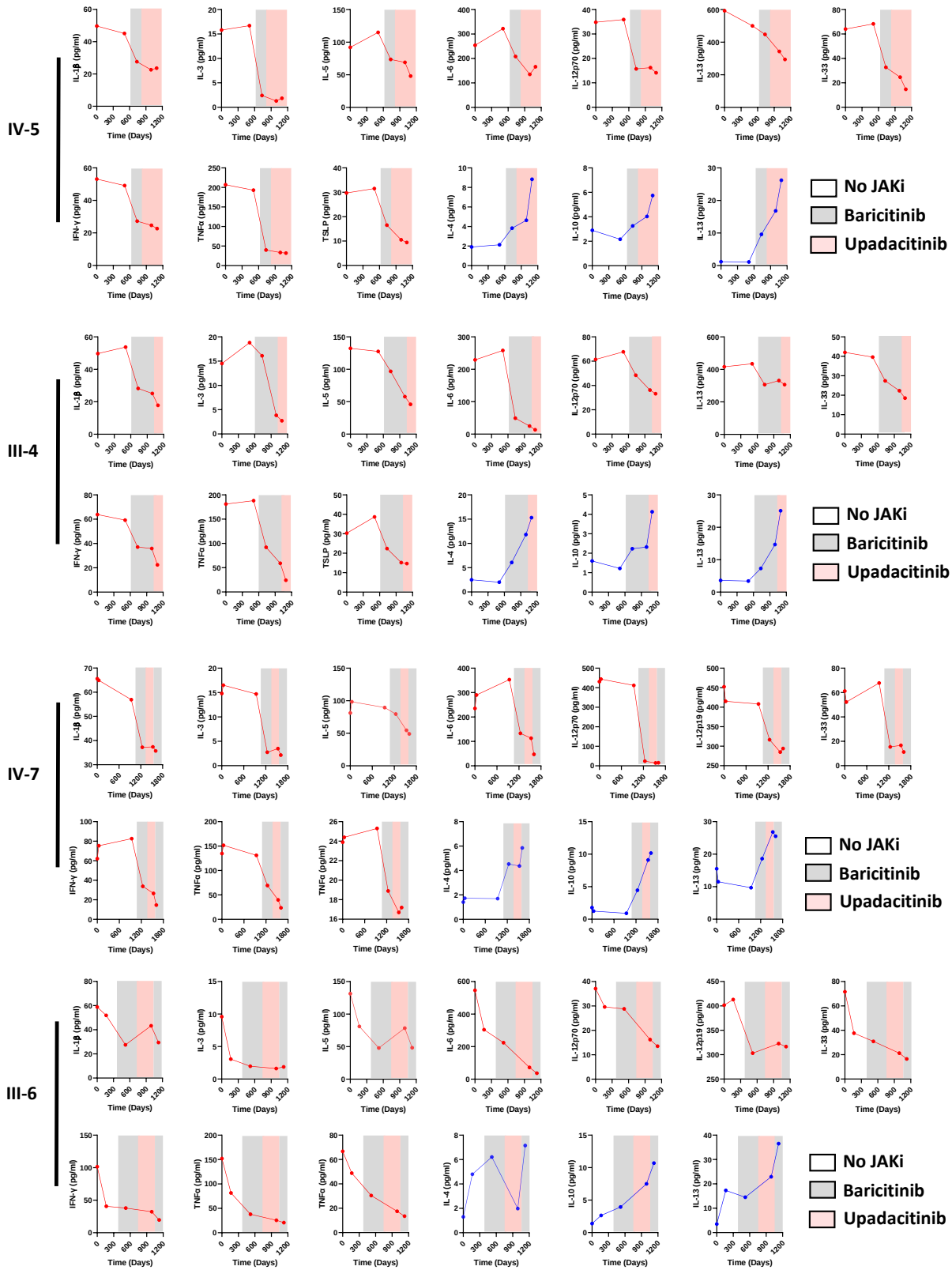

Figure S16: Cytokine profile in patients successively treated with baricitinib and upadacitinib. Representation of the evolution of the circulating levels of cytokines in patients before the initiation of treatment with JAK inhibitors and during treatment with baricitinib (grey) or upadacitinib (light red).

Sup Fig 17

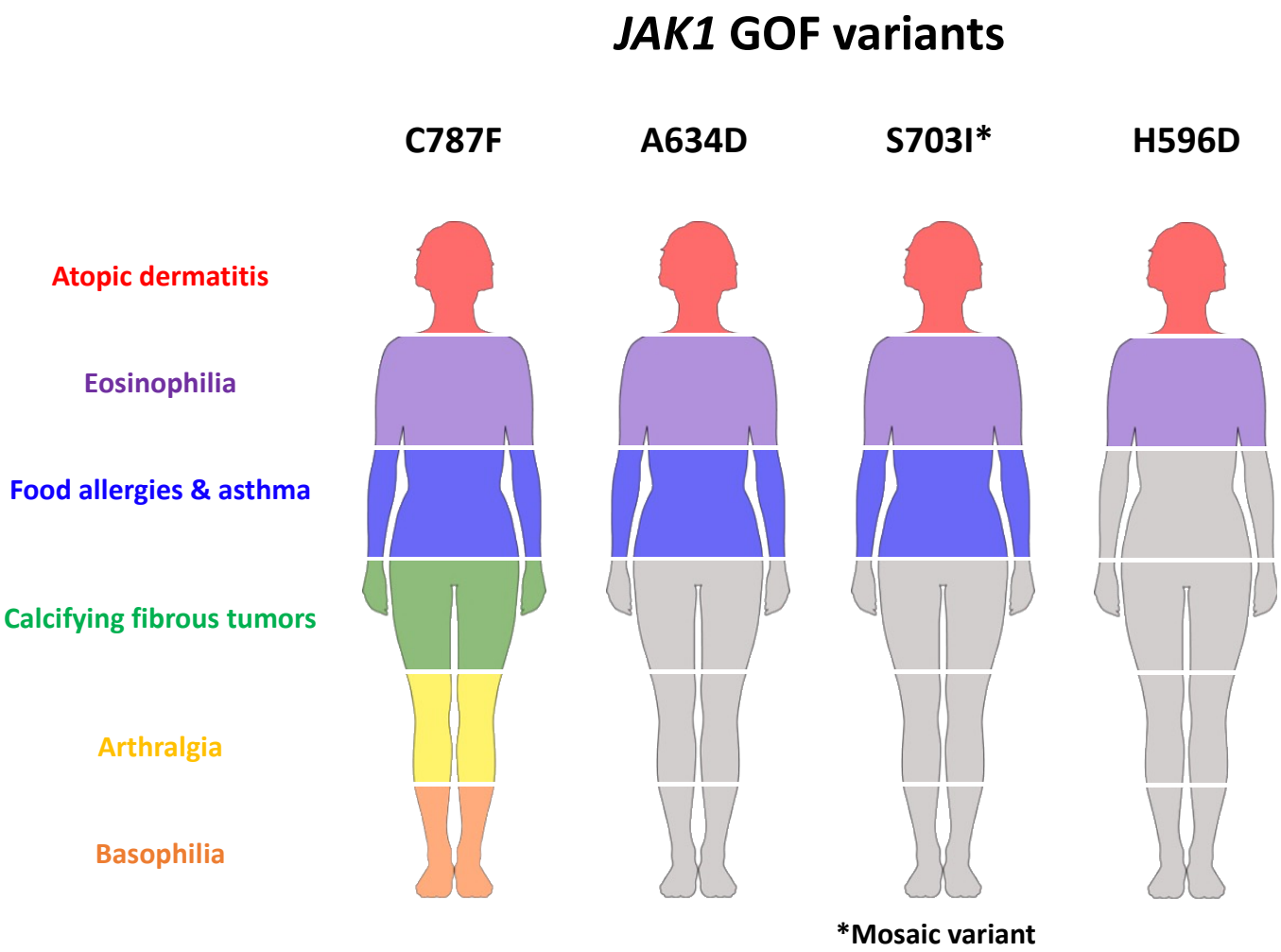

Figure S17: Phenotypic overlap of JAK1^{C787F} with other JAK1 GOF variants
Based on Del Bel et al. J Allergy Clin Immunol. 2017 and Biggs et al. JCI Insight. 2022 (A634D), Grubber et al. Immunity. 2020 (S703I) and Takeichi et al. Front Immunol. 2021 (H596D). Also, notable clinical features encountered in the other JAK1 GOF variants included membranous nephropathy (S703I), hepatitis (H596D) and autism (H596D).

Sup Fig 18

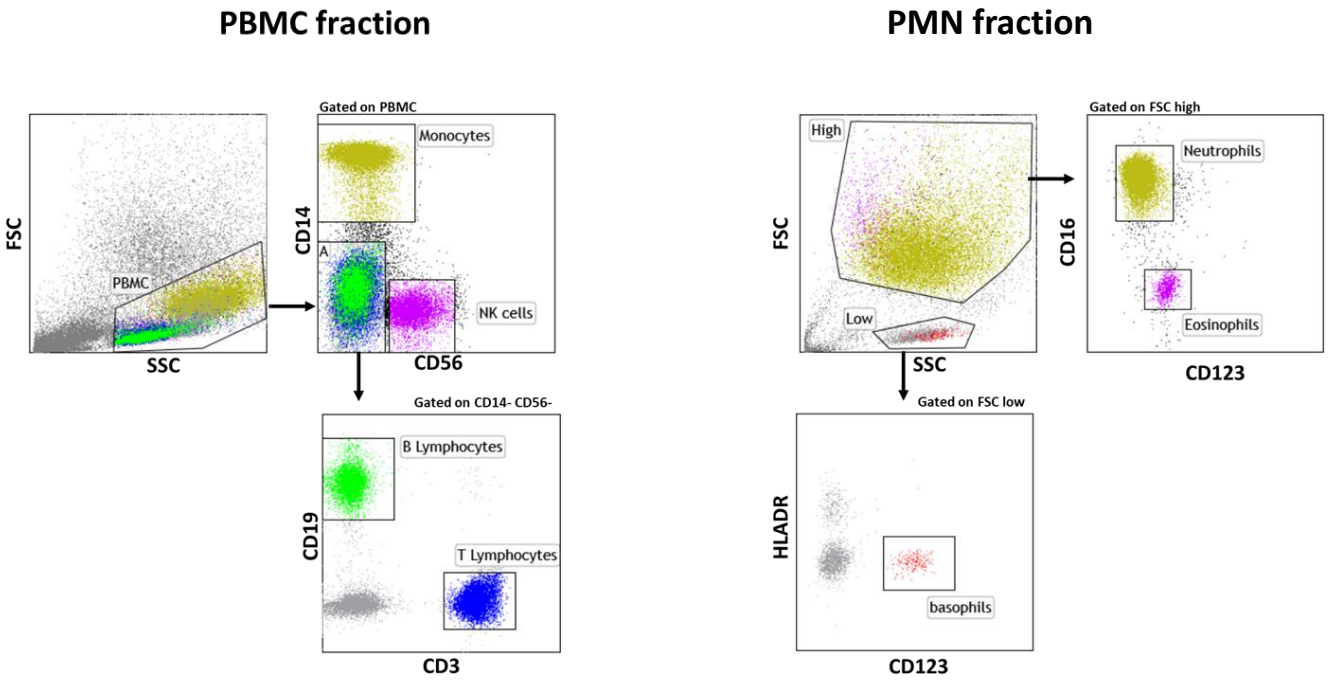

Figure S18: Gating strategy for cell sorting

III. Supplementary Tables

Table S1 : Clinical findings

Patient N°	II-16	III-4	III-6	III-13	IV-5	IV-7	IV-9	V-1	V-2
Sex	F	F	M	F	M	F	F	M	M
Age on study (years old)	69†	56	53	56	30	23	27	3	1
Previous diagnosis	Atopic eczema Seronegative polyarthritis and severe asthma	Ichthyosis	Sarcoidosis	Ichthyosis	Addison's disease Eczema and atopic dermatitis	Crohn-like disease with spondylarthritis and neutrophilic dermatosis	Atopic dermatitis	Severe eczema	Not done
Failure to thrive / short stature	YES	NO	NO	NO	YES	NO	NO	YES	YES
Cutaneous features	Ichthyosis	Ichthyosis	Ichthyosis	Ichthyosis Atopic dermatitis	Ichthyosis Atopic dermatitis	Ichthyosis Atopic dermatitis Sweet syndrome	Ichthyosis Atopic dermatitis	Ichthyosis Atopic dermatitis	Ichthyosis Atopic dermatitis
Digestive features		Chronic watery diarrhea	Chronic watery diarrhea Food allergies	Chronic watery diarrhea	Chronic watery diarrhea Food allergies	Chronic diarrhea with occasional bleeding Ileitis Food allergies	Food allergies	Constipation with overflow Encopresis Anorexia Food allergies	Food allergies
Musculoskeletal features		Arthralgia	Arthralgia	Arthralgia	Arthralgia	Polyarthralgia			
Other clinical features	Severe asthma			Severe asthma	Adrenal insufficiency	Flushes Recurrent fevers		Major growth retardation	Major growth retardation
Calcified tumors	Yes	Yes	Yes	Yes	Yes	Yes	Yes	No	Unknown
CRP (N<5mg/L	10	13.2	9.6	15.7	11.3	52	25	1	N
Hemogram	Mild PME elevation	Mild PMB elevation	Mild PMN & PMB & PME elevation	Mild	Mild PMN & PMB elevation	Mild PMN & PMB elevation	Mild PMN & PME elevation	Mild	Mild PME elevation

				PMN & PMB & PME elevation				PMN & PMB & PME elevation	
Gammaglobulin (g/L)	6	6.6	7.2	7.2	8.6	6.2	~~3.8~~ 8.8	4.0	2.6
IgG / IgA / IgM (g/L) Bold = decreased*	**4.6** / 2.2 / **0.4**	6.5 / 3.0 / 0.59	6.7 / 3.6 / 1.1	7.8 / 2.2 / 0.7	6.8 / 2.1 / 0.9	**6.2** / 2.0 / 1.1	8.7 / 1.4 / 2.5	**3.9** / 0.5 / 0.5	**2.0** / x / x
IgE (UI/L) Bold = elevated for age	5	11	91	**1241**	**667**	26	**478**	**4488**	76.2
Blood Tryptase rate N<15 µg/L	4.2	3.4	5.5	3.3	6.6	3.7	3,8	3	ND
Blood histamine (nmol/L) N<700	1233	1725	3712	2720	4122	2256	4050	3958	3493
Previous treatments	Emollients, antiH, inhaled CS	Emollients, antiH, montelukast	Emollients, antiH, montelukast, ADA	Emollients, antiH, montelukast, inhaled CS	Emollients, antiH, montelukast, hydrocortisone,	Emollients antiH, montelukast, mesalazine, systemic CS, AZA MTX, IFX, ADA, USM, OMA	Emollients, antiH, topical CS	Emollients, antiH, topical CS	Emollients, antiH, topical CS

Abbreviations: F: female; M: male; ND: not done; PMN, Polymorphonuclear Neutrophil; PMB: Polymorphonuclear basophil; PME: Polymorphonuclear eosinophil; antiH: antihistamines; CS: corticosteroids; ADA: adalimumab; AZA: azathioprine; MTX: methotrexate; IFX: infliximab; USM: ustekinumab; OMA: omalizumab

*Normal ranges for gammaglobulins:

- Adults = IgG: [6.5-12.0] g/L; IgA: [1.0-3.2] g/L; IgM [0.5-3.0]
- Child 1-2 years = IgG: [3.1-13.8] g/L; IgA: [0.3-1.2] g/L; IgM [0.5-2.2]
- Child 3-6 years = IgG: [4.9-16.1] g/L; IgA: [0.4-2.0] g/L; IgM [0.5-2.0]

†: deceased

Table S2: Auto immunity screening

		II-16	III-4	III-6	III-13	IV-5	IV-7	IV-9	V-1	V-2	V-4
Nuclear	**ANA**	-	-	-	-	1/160 *	-	-	1/160	-	-
Tissue	**ASMA**	-	-	-	-	-	-	-	-	-	-
	AMA	-	-	-	-	-	-	-	-	-	-
	ANA	-	-	-	-	-	-	-	-	-	-
	Anti LKM1	-	-	-	-	-	-	-	-	-	-
	APCA	-	-	-	-	-	-	-	-	-	-
	Anti LC1	-	-	-	-	-	-	-	-	-	-

ANA: anti-nuclear antibodies, ASM: anti-smooth muscle antibodies, AMA: anti-mitochondrial antibodies, APCA: anti-parietal cells antibodies; *(type DFS70)

Table S3: Treatment information for samples with cytokines dosages

				Cytokines (pg/ml)												
Patients	Immunomodulatory treatment	Dose	ttt duration (Days)	IL1b	IL3	IL4	IL5	IL6	IL10	IL12 (p70)	IL13	IL23 (p19)	IL33	INFg	TNFa	TSLP
II-16	-			33,4	23	4,25	78,1	145,2	2,33	38,6	2,28	677,5	65,2	41,3	247	32,5
III-13	-			52,5	16,9	2,13	73,7	321	1,25	43,8	4,08	452,6	59,9	44,2	155	38,8
III-13	Baricitinib	2 mg x2/j	452	20,1	2,85	7,84	52,3	35,7	3,17	29,9	15,1	336,1	26,1	23,6	37,2	14,8
III-4	-			53,7	18,8	2,01	127,5	258	1,22	67,7	3,4	434,5	39,6	59,2	188	38,7
III-4	Baricitinib	2 mg/j	229	28,2	16,1	6,08	96,8	49,2	2,23	48,4	7,3	306,1	27,4	37,1	92,1	22,4
III-4	Baricitinib	2 mg/j	487	25,1	3,84	11,82	57,8	24,8	2,32	36,2	14,7	331,4	22,3	35,9	59,1	15,2
III-4	Upadacitinib	30 mg/j	114	17,8	2,73	15,3	45,9	13,4	4,13	33,2	25,1	306,4	18,5	22,4	24,2	14,7
III-6	-			51,9	3,07	4,8	81	304	2,65	29,6	17,3	413,1	37,6	40,7	81,6	48,8
III-6	Baricitinib	2 mg x2/j	117	27,5	1,97	6,21	47,9	224	3,94	28,8	14,5	303	30,9	37,9	37,9	30,4
III-6	Upadacitinib	30 mg/j	58	43,3	1,62	1,98	78,4	72	7,5	16,2	22,9	322,8	21,2	32,3	25,5	17,5
III-6	Upadacitinib	4 mg/j	99	29,4	1,87	7,15	48,3	36,8	10,7	13,5	36,5	316,6	16,5	19,7	20,8	13,5
IV-5	-			45,1	16,7	2,13	115	322	2,16	35,9	1,12	500	68,3	49,1	193	31,5
IV-5	Baricitinib	2 mg x2/j	436	27,6	2,4	3,83	73,51	208	3,26	15,7	9,6	447,6	32,7	27,2	39,9	16,5
IV-5	Upadacitinib	30 mg/j	10	22,6	1,29	4,64	69	135	4,03	16,2	16,8	343,1	24,6	24,7	33,4	10,5
IV-5	Upadacitinib	30 mg/j	122	23,6	1,84	8,84	48,1	166	5,74	14,1	26,2	294	14,7	22,7	32	9,4
IV-7	Infliximab	10 mg/kg/6w	486	65,6	14,8	1,41	81,2	235	1,78	431	15,5	452,4	61,2	62,1	134,8	23,9
IV-7	Infliximab	10 mg/kg/6w	528	64,9	16,5	1,73	98,4	290	1,24	444	11,5	415,2	52,2	75,4	151,6	24,4
IV-7	Baricitinib	2 mg x2/j	250	37,2	2,76	4,53	79,5	133	4,45	24	18,6	316,5	15,4	33,8	69,3	18,9
IV-7	Upadacitinib	30 mg/j	58	37,4	3,51	4,37	54,5	113	9,11	14,6	26,8	284,8	16,7	26,5	39,7	16,7
IV-7	Baricitinib	4 mg/j	135	35,7	2,18	5,85	49,1	47,2	10,17	15,5	25,5	294	11,2	14,6	23,5	17,2
IV-9	-			42,4	7,4	3,33	61,7	191	1,19	38,7	2,76	452	57,4	53,5	201	64,7
V-1	-			55,3	15,3	1,33	61,6	307	1,47	58,1	3,36	4546	96,1	60,3	67,1	25,7
V-1	Baricitinib	2 mg/j	288	57,5	12,9	1,38	93	353	1,14	47,3	3,48	519,4	86,1	66,1	71,7	25,1
V-1	Baricitinib	2 mg/j	400	54,8	17,7	1,35	131,5	293	1,27	55,6	1,68	539,5	20,5	51,2	85,2	28,6
V-4	-			37,5	16,2	3,9	62,61	194	1,89	40,7	4,33	497	42,5	48,4	135	44,6
HD1				6,21	1,34	2,03	36,9	1,64	4,42	14,8	23,5	162	2,46	13,1	26,4	4,2
HD2				3,05	1,33	6,46	38,2	2,23	15,3	14,3	14,5	207	3,54	13,9	17,2	9,7
HD3				4,54	1,36	1,91	32,7	1,57	4,87	12,6	14,2	166	2,1	16,1	14,2	8,1
HD4				4,87	0,83	4,08	32,2	1,68	6,8	14,1	16,7	239	1,9	7,9	18,2	7,8
HD5				1,85	1,49	4,57	29,6	3,63	14,8	18,9	13,7	162	4,28	13,7	26,5	9,1
HD6				4,09	1,38	4,29	40,2	2,21	13,5	13,6	16,2	239	8,1	14,2	24,6	4,5
HD7				2,59	1,97	3,5	35,2	2,58	5,97	12,5	22,4	159	9,5	12,8	30,9	7,2
HD8				2,24	1,42	2,84	34,3	3,43	12,4	13,4	23,9	225	3,41	15,1	21,8	3,5

Table S4: List of fluorochrome-conjugated antibodies used for membrane antigen staining

Target	**Fluorochrome**	**Clone**	**Manufacturer**
Mix 1			
CD14	APC-AF750	RMO52	Beckman Coulter
CD16	PEAF610	eBloCB16	Life technologies
CD3	APC	REA613	Miltenyi Biotec
CD8	AF405	3B5	Invitrogen
CD19	AF700	HIB19	Life technologies
IgD	PEVio770	REA740	Miltenyi Biotec
CD56	SB702	TULY56	Life technologies
Mix 2			
CD14	APC-AF750	RMO52	Beckman Coulter
CD16	PEAF610	eBloCB16	Life technologies
CD3	PE-Cy-5.5	SK7	Life technologies
CD8	AF405	3B5	Invitrogen
CD19	AF700	HIB19	Life technologies
IgD	PEVio770	REA740	Miltenyi Biotec
CD56	SB702	TULY56	Life technologies
CD123	APC	6H6	Life technologies
CD4	eFluor506	RPA-T4	Life technologies

Table S5: List of metal-isotope-tagged antibodies used for mass cytometry

Target	**Label**	**Clone**	**Manufacturer**
CD45	089Y	HI30	Fluidigm
CD196 (CCR6)	141Pr	G034E3	Fluidigm
CD19	142Nd	HIB19	Fluidigm
CD123	143Nd	6H6	Fluidigm
CD38	144Nd	5HIT2	Fluidigm
CD38	172Yb	5HIT2	Fluidigm
CD4	145Nd	RPA-T4	Fluidigm

CD8	146Nd	RPA-T8	Fluidigm
CD11c	147Sm	Bu15	Fluidigm
CD194 (CCR4)	149Sm	L291H4	Fluidigm
pSTAT5B	150Nd	47	Fluidigm
CD66b	152Sm	80H3	Fluidigm
pSTAT1	153Eu	4a	Fluidigm
CD3	154Sm	UCHT1	Fluidigm
CD27	155Gd	L128	Fluidigm
pSTAT3	158Gd	4/P-Stat3	Fluidigm
CD197 (CCR7)	159Tb	G043H7	Fluidigm
CD14	160Gd	M5E2	Fluidigm
CD183 (CXCR3)	163Dy	G025H7	Fluidigm
pNF-kB	166Er	K10-895.1	Fluidigm
pSTAT6	168Er	18	Fluidigm
CD45RA	170Er	HI100	Fluidigm
HLA-DR	173Yb	L243	Fluidigm
pSTAT4	174Yb	38	Fluidigm
CD56	176Yb	NCAM16.2	Fluidigm
CD16	209Bi	3G8	Fluidigm